Mathematical modeling of gas-phase hydrogen storage: equilibrium kinetics approach.

A. Ledovskikh[1], D. Danilov[2] and P.H.L. Notten[1,3,*]

[1] *Eindhoven University of Technology, Den Dolech 2, 5600 MB Eindhoven, The Netherlands*

[2] *Eurandom, Den Dolech 2, 5600 MB Eindhoven, The Netherlands*

[3] *Philips Research Laboratories, Prof. Holstlaan 4, 5656 AA Eindhoven, The Netherlands*

A new equilibrium kinetic model has been developed, describing the hydrogen storage in hydride-forming materials. Using reasonable structural assumptions and based on first-hand principles of chemical kinetics and statistical thermodynamics model is capable to describe complex process in the hydrogen storage system including phase transition. A complete set of equations, describing pressure-composition isotherms in both solid-solution and two-phase coexistence regions have been obtained. Basing on energy conception and principles of statistical thermodynamics, generalization of Langmuir, Temkin and other kinetic approaches has been made. Explicit, general and universal algorithm of rate constants determination using well-defined phase-dependent Hamiltonians for bulk and surface of the hydride forming material has been proposed. Various characteristics of both model ($LaNi_yCu_{1.0}$) and commercial, MischMetal-based, AB_5-type materials at different compositions and temperatures have been simulated. Good agreement between experimental and theoretical results for the pressure-composition isotherms obtained in the gas-phase experiment has been found in all cases.

[*] To whom correspondence should be addressed (Peter.Notten@Philips.com)

1. INTRODUCTION

Modern society urgently needs for clean renewable and efficient energy storage devices. Sustainable energy suppliers have to promote a sustainable economic development and quality of life as well as for environment protection. MetalHydride (MH) compounds are successfully employed as efficient hydrogen storage via the gas phase, and this is one of the key factors, enabling usage of hydrogen-driven Fuel Cells and other ecologically clean portable applications. The second application of the MH materials is high energy density, Nickel MetalHydride (NiMH) batteries, nowadays widely applied in many portable electronics and Hybrid Electrical Vehicles (HEV).[1-6]

Hydrogen storage is highly complex multistage process. The first step of hydrogen storage is dissociation of hydrogen molecules at the interface between metal and gas phase. This represents an adsorption process. The process which is reverse to that is a recombination of adsorbed hydrogen atoms. The adsorbed hydrogen atoms may penetrate the interstitial sites inside of the hydride-forming material, what substitute an absorption process. The absorbed hydrogen atoms spread inside the bulk of the material due to diffusion. The overall reaction can be represented by

$$M + \tfrac{1}{2} H_2 \leftrightarrow MH \ . \qquad (1)$$

Evidently, a chemical equilibrium exists between hydrogen stored in the solid and that present in the gas phase, which is generally characterized by pressure-composition isotherms.[3-7]

A typical pressure-composition absorption isotherm and accompanying phase diagram are schematically shown in curve (a) and (b) of Fig. 1, respectively[7-11]. During hydrogen absorption at low concentrations, a solid solution is formed, which is generally denoted as the α-phase. In this concentration region the partial hydrogen pressure ($P_{H_2}^{eq}$) is clearly dependent on the amount of stored hydrogen. After the hydrogen concentration has reached a certain critical value (x_α), phase transition occurs and the α-phase is continuously transformed into the β-phase. The pressure dependence in this two-phase coexistence region is generally characterized by a (sloping) plateau[7,12,13]. Phase transition

is completed at x_β and a solid solution is subsequently formed by the β-phase only. This typical three-step process will play an important role in the present paper.

Hydrogen absorption reaction (Eq.1) is a complex process. We can trace a number of attempts to describe the adsorption process from pure thermodynamics viewpoint. The majority of the existing thermodynamic models employ methods of statistical mechanics, which derives macroscopic characteristics, such as Gibbs free energy and entropy, from a microscopic description of the system. Lacher[14] has proposed one of the first models of that kind. His ideas were further developed in Lototsky *et al*.[15] paper. Both models happen to be not suitable for description of the sloping plateaus. Naito *et al*.[16] proposes a lattice gas model to describe pressure-composition isotherms with sloping plateaus. However, this model demonstrates a poor fit between the experimental and simulation results. Recently a new statistical Lattice Gas Model (LGM) has been proposed[13]. This model is based on first principles of statistical mechanics and takes into account the hydrogen absorption and desorption in hydride-forming materials in both solid solution and two-phase coexistence regions.

All abovementioned papers concentrate only on thermodynamic of the process. No kinetic limitations are considered. However chemical kinetic imposes additional limitations on equilibrium. Thus the shape of pressure-composition isotherms and equilibrium potential curves is affected. To describe complex processes taking place in operating fuel cell one needs to know complete kinetics of hydrogen storage, i.e. adsorption, absorption and recombination. In this case pure statistical thermodynamic description is not enough to describe these stages and chemical kinetic approach must be used.

There are a number of papers discussing various aspects of hydrogen storage kinetics. Martin et al. consider absorption and desorption kinetic of hydrogen. They proposed very detailed scheme of hydrogen storage reaction but did not addressed equilibrium situation. Same drawback suffers Fernandez et al. and Feldman et al. We know only few attempts to describe equilibrium kinetics of complex systems. One of the first and fundamental works is Gileadi[17-18]. Author deeply described similar system, considered various (electro-)chemical stages of the process and different kinetic approaches to the rate constant determination (Langmuir, Temkin, ect.). But system considered by Gileadi is very different from MH storage system and some of kinetic equations were done as empirical. The first attempt of description of hydrogen storage system from kinetics point of view has been made by Feng et. al.[19]. Authors applied

equilibrium kinetics approach to describe pressure-composition isotherms and obtained good agreement with experimental data. However their description of phase transition and hydrogen surface recombination are oversimplified and rate constants are treated in empirical way. We improve the chemical description of the overall reaction significantly considering proper hydrogen recombination reaction and letting reaction rates vary in different phases.

In the present paper, a new equilibrium kinetic model is proposed. This model is based on first principles of chemical kinetics and statistical mechanics and takes into account the hydrogen absorption and desorption in hydride-forming materials in both solid solution and two-phase coexistence regions. We provided universal and systematic approach to the activation energies and rate constants determination using well-defined phase-dependent Hamiltonians for bulk and surface of the hydride forming material. Proposed approach, definitely, can be extended for arbitrary reacting system. The simulated development of partial hydrogen pressure was compared with wide range of experimental results, showing very good agreement.

2. MODEL

A. System description.

Let us consider storage reaction via the gas phase in more details (Fig.2). The hydrogen atoms are chemically adsorbed at the surface and then converted to absorbed state in the first atomic layer which is also called sublayer or subsurface [Schlapbach]. Then hydrogen moves to the bulk of material by usual diffusion. Simultaneously recombination of adsorbed hydrogen atoms takes place at the surface of the hydride-forming material. In Fig.2 θ is the normalized surface coverage, x is the normalized hydrogen concentration in the first atomic layer of the hydride-forming material, a_g is the hydrogen concentration in the gas phase. Thus, two reaction steps must be considered:

1. Hydrogen recombination/dissociation (Tafel) reaction:

$$2M^s + H_{2(g)}\,(a_g) \underset{k_{-1}}{\overset{k_1}{\rightleftharpoons}} 2MH_{ad}\,(\theta) \qquad (2)$$

2. Hydrogen absorption/adsorption reaction:

$$M^s + MH_{ad}(\theta) \underset{k_{-2}}{\overset{k_2}{\rightleftharpoons}} MH_{abs}(x) + M^s \qquad (3)$$

For the gas phase we adopt Boltzmann equation, linking pressure ($P_{H_2}^{eq}$) and concentration (a_g) of the hydrogen for given temperature (T):

$$P_{H_2}^{eq} = a_g RT \ . \qquad (4)$$

In fact we will consider general reactions described by Eqs. (2-3) separately within each phase. We will assume that reaction flows in each phase independently on other phase.

B. Model basics. Structural assumptions.

Let us consider crystallographic structure of the bulk of MH material. A well-known class of hydrogen storage alloys, nowadays exclusively applied in rechargeable NiMH batteries, is the so-called AB_5-type compounds. A schematic representation of the hexagonal unit cell of a non-stoichiometric representative of this class is shown in Fig.3(a)[18-20]. The crystallographic structure is composed of large A-type atoms (*e.g.* La) at the as-denoted 1a positions and smaller B-type atoms (*e.g.* Ni, Co) surrounding them in a well-defined way at the 3g, 2c and 6l positions. Deviation from the stoichiometric composition was proven to take place by introducing dumbbell-pairs of B-type atoms at some A-type (2e) positions[20,21]. Upon hydrogenation the hydrogen guest atoms will occupy certain well-defined interstitial sites in the open AB_5-host structure, which can be recognized in the cross-section of Fig.3(b). It is assumed that a single guest atom can only occupy one host site and that each unit cell may have several host sites. Since the host material can be in more than one crystallographic state, different unit cells, each characterized by its own specific number of host sites, have to be considered.

Consider the hydrogen storage system consisting of the gas phase, the surface layer of dissociated hydrogen atoms and the bulk of hydrogen storage material. Suppose that the bulk of hydrogen storage material consists of M^b unit cells, each of those can, upon hydrogen storage, be either in the α- (M_α^b) or the β-state (M_β^b), leading to

$$M^b = M_\alpha^b + M_\beta^b$$

When the crystallographic structure of both phases is assumed to be identical, M^b remains constant throughout the hydrogenisation process. We assumed that the number of host sites per unit cell for the α- and β-phase are equal. This number is denoted as d^b. The total number of host sites in the solid (N^b) can then be obtained from

$$N^b = N_\alpha^b + N_\beta^b = d^b M_\alpha^b + d^b M_\beta^b .$$

The amount of hydrogen guest atoms in the α- and β-phase is denoted by n_α^b and n_β^b, respectively, where the total number of occupied hydrogen sites (n^b) is given by the summation of n_α^b and n_β^b. Denote $n_{\max}^b$ the maximal number of host sites in the bulk that can be occupied by hydrogen. Then, the normalized number of absorbed hydrogen atoms x (which is also called state of charge) in the system can be represented by

$$x = \frac{n^b}{n_{\max}^b} = \frac{n_\alpha^b + n_\beta^b}{n_{\max}^b}. \tag{5}$$

The curves in Fig 4(a) and 4(b) show the development of the normalized number of host sites $N_i^b / n_{\max}^b$ as a function of the hydrogen content in the various phases (i) of the bulk material. The dependence of N_α^b and N_β^b on x in the three crystallographic regions can be mathematically represented as

$$N_\alpha^b = \begin{cases} d^b M^b, & x < \mathrm{x}_\alpha \\ d^b M^b \left(\dfrac{\mathrm{x}_\beta - x}{\mathrm{x}_\beta - \mathrm{x}_\alpha} \right), & \mathrm{x}_\alpha \le x \le \mathrm{x}_\beta \\ 0, & x > \mathrm{x}_\beta \end{cases}; \quad N_\beta^b = \begin{cases} 0, & x < \mathrm{x}_\alpha \\ d^b M^b \left(\dfrac{x - \mathrm{x}_\alpha}{\mathrm{x}_\beta - \mathrm{x}_\alpha} \right), & \mathrm{x}_\alpha \le x \le \mathrm{x}_\beta \\ d^b M^b, & x > \mathrm{x}_\beta \end{cases} \tag{6}$$

In curves Fig. 4(c) and (d) the development of the normalized number of absorbed guest hydrogen atoms ($n_i^b / n_{\max}^b$) is shown. At low hydrogen concentration the hydrogen atoms fill the available α-sites only. The maximum concentration level within α-phase is

reached at $x = \mathrm{x}_\alpha$. The phase transition starts at that point and n_α^b decreases linearly in the two-phase coexistence region. Finally n_α^b became zero and the phase transition ends at x_β. We assume that all available host sites are fully occupied by hydrogen atoms at $x = 1$, that is $n_\beta^b = N_\beta^b = n_{\max}^b$ at that point. The following expressions, therefore, determine evolution of n_α^b and n_β^b as function of x

$$n_\alpha^b = \begin{cases} x n_{\max}^b, & x < \mathrm{x}_\alpha \\ \mathrm{x}_\alpha\, n_{\max}^b \left(\dfrac{\mathrm{x}_\beta - x}{\mathrm{x}_\beta - \mathrm{x}_\alpha} \right), & \mathrm{x}_\alpha \le x \le \mathrm{x}_\beta \\ 0, & x > \mathrm{x}_\beta \end{cases}; \; n_\beta^b = \begin{cases} 0, & x < \mathrm{x}_\alpha \\ \mathrm{x}_\beta\, n_{\max}^b \left(\dfrac{x - \mathrm{x}_\alpha}{\mathrm{x}_\beta - \mathrm{x}_\alpha} \right), & \mathrm{x}_\alpha \le x \le \mathrm{x}_\beta \\ x n_{\max}^b, & x > \mathrm{x}_\beta \end{cases} \qquad (7)$$

It is clear that at low hydrogen concentrations whole volume of the sample is occupied by α-phase. When the phase transition starts, volume of α-phase decreases linearly in favor of β-phase and diminishes at x_β. In the following derivations it is convenient to use variable v_i that denotes the percentage of total host sites of hydride forming material related to particular phase. This variable formally defines as

$$\mathrm{v}_\alpha = \begin{cases} 1, & x < \mathrm{x}_\alpha \\ \dfrac{\mathrm{x}_\beta - x}{\mathrm{x}_\beta - \mathrm{x}_\alpha}, & \mathrm{x}_\alpha \le x \le \mathrm{x}_\beta \\ 0, & x > \mathrm{x}_\beta \end{cases}; \qquad \mathrm{v}_\beta = \begin{cases} 0, & x < \mathrm{x}_\alpha \\ \dfrac{x - \mathrm{x}_\alpha}{\mathrm{x}_\beta - \mathrm{x}_\alpha}, & \mathrm{x}_\alpha \le x \le \mathrm{x}_\beta \\ 1, & x > \mathrm{x}_\beta \end{cases}. \qquad (8)$$

Apparently, if we denote the total volume of the sample as V_0 then volume occupied by phase i is expressed as $V_i = V_0 \mathrm{v}_i$ (we neglect change in the volume of the unit cell during phase transition)). In similar way we can express numbers of available host sites in each phase i.e. $N_i^b = d^b M^b \mathrm{v}_i$. The *normalized concentration* of the hydrogen in particular phase i is defined as

$$x_i = n_i^b / N_i^b . \qquad (9)$$

We will also define the *partial hydrogen concentrations* in phase i as

$$x^i = n_i^b / n_{\max}^b . \qquad (10)$$

Note that $x = x^\alpha + x^\beta$, but $x \neq x_\alpha + x_\beta$. The average concentration of hydrogen in the sample is not equal to sum of hydrogen concentrations in each of phases, unless we have just one phase. In the case of pure phase the partial concentration coincides with usual normalized concentration.

Now let us consider the surface layer of the hydride-forming material. The surface layer is composed of half-opened unit cells that contain places suitable for hosting of hydrogen atoms. We are working with quasi-one-dimensional model and we assume unit half-cells at the surface belong to the same phase as all unit cells exactly below the surface. However the total number of surface unit cells M^s remain unchanged and

$$M^s = M_\alpha^s + M_\beta^s .$$

We assumed that the number of host sites per (surface) unit cell for the α- and β-phase are equal and denoted as d^s. The total number of host sites at the surface (N^s) can then be obtained from

$$N^s = N_\alpha^s + N_\beta^s = d^s M_\alpha^s + d^s M_\beta^s .$$

Consider the surface area occupied by particular phase at the surface. This surface area will be denoted as $A_i, i = \alpha, \beta$. We assume that fraction of each phase (α or β) at the surface is exactly the same as beneath in the bulk, and, therefore can be expressed as

$$A_i = A_0 \mathrm{v}_i , \qquad (11)$$

where A_0 is the total sample surface area. It immediately follows $N_i^s = d^s M^s \mathrm{v}_i$.

Denote n_α^s and n_β^s the numbers of adsorbed hydrogen atoms at the surface of the α and β phases accordingly. Denote $n_{\max}^s$ the maximal number of host sites in the surface layer that can be occupied by hydrogen. Again, like in the case of bulk we assume this

number doesn't depend on x (in fact $n^s_{\max} = d^s M^s$). Then, by definition, the *total surface coverage* of the surface of the hydride-forming material is:

$$\theta = \frac{n^s_\alpha + n^s_\beta}{n^s_{\max}}.$$

The physical sense behind this definition is simple θ is a fraction (percentage) of the total number of available host sites that are occupied by the hydrogen atoms. Define the i-th phase *surface coverage* as fraction of occupied host sites at the surface of i-th phase i.e.

$$\theta_i = n^s_i / N^s_i . \tag{12}$$

For mathematical convenience we will define also *partial surface coverages* for each phase as

$$\theta^i = n^s_i / n^s_{\max} . \tag{13}$$

Apparently the total surface coverage is a sum of both partial $\theta = \theta^\alpha + \theta^\beta$. Note that for particular phase the surface coverage indicates percentage of filled host sites relative to the number of host sites available within the same phase, while the partial surface coverage show percentage of filled host sites relatively to the total number of host sites in whole surface, i.e. in both phases together. Considering Eqs. 12-13 together with Eqs. 6-8 we can see that $\theta^i = \theta_i \mathrm{v}_i$.

C. Reaction kinetic description

Schematic representation of hydrogen recombination/dissociation (Eq.2) and adsorption/absorption (Eq.3) processes using conception of phase separation is shown in Fig.5. According to that scheme we can split our system into two parts.

Part 1. Hydrogen dissociation/recombination reaction. According to the reaction scheme (Eq.2, Fig.3,4) and basic principles of chemical kinetics we can write dissociation (J^i_1) and recombination (J^i_{-1}) fluxes in phase i [mol/s] as

$$\begin{cases} J_1^i = \overline{k}_1^i \, A_i \left[a_i^s(M) \right]^2 a_g \,, \\ J_{-1}^i = \overline{k}_{-1}^i \, A_i \left[a_i^s(MH) \right]^2 \,, \end{cases} \quad i = \alpha, \beta \tag{14}$$

where $\overline{k}_1^i$, $i = \alpha, \beta$ [$m^5 mol^{-2} s^{-1}$] is normalized dissociation rate constant, $\overline{k}_{-1}^i$, $i = \alpha, \beta$ [$m^2 mol^{-1} s^{-1}$] is the normalized recombination rate constant, A_i [m^2] is the surface area attributed to phase i, $a_i^s(M)$ [mol m^{-2}] is the surface activity of free host sites in phase i, $a_i^s(MH)$ [mol m^{-2}] is the surface activity of occupied host sites in phase i and a_g [mol m^{-3}] is the hydrogen activity in the gas phase. For simplicity we assume that all activities are equal to corresponding concentrations. If we accept the assumption that chemically active species are homogeneously distributed across the surface, occupied by particular phase, then we can express concentrations of relevant species via surface coverages (Eq. 12), in the following way. Denote a_0^s the surface density of available host sites (same in both phases for scarcity). Consider $a_i^s(MH)$. This is surface concentration of occupied host sites (MH_{ad}) in phase i. Then, by definition of surface coverage

$$a_i^s(MH) = a_0^s \, \theta_i \,.$$

In similar way, $a_i^s(M)$ is the surface concentration of free host sites in i-th phase. By definition of a_0^s we have $a_i^s(M) + a_i^s(MH) = a_0^s$, therefore

$$a_i^s(M) = a_0^s (1 - \theta_i) \,.$$

Dividing the fluxes onto the total surface area A_0 and using definition (11) we obtain rates (fluxes per unit area) of dissociation (r_1^i) and recombination (r_{-1}^i) reactions [mol $s^{-1} m^{-2}$]:

$$\begin{cases} r_1^i = k_1^i \mathrm{v}_i (1 - \theta_i)^2 a_g \,, \\ r_{-1}^i = k_{-1}^i \, \mathrm{v}_i (\theta_i)^2 \,, \end{cases} \quad i = \alpha, \beta \tag{15}$$

where $k_1^i = \bar{k}_1^i \left[a_0^s \right]^2$, $i = \alpha, \beta$ is the dissociation rate constant [s^{-1}] and $k_{-1}^i = \bar{k}_{-1}^i \left[a_0^s \right]^2$, $i = \alpha, \beta$ is the recombination rate constant [mol $s^{-1}m^{-2}$]. These rate constants differ from normalized rate constants ($\bar{k}_j^i$) by squared concentration of surface host sites.

Phases at the surface (Fig.5) are separated but hydrogen concentration (pressure) in the gas phase is the same for both phases. In chemical equilibrium rates of direct and inverse reactions must coincide, thus we can write balance equation:

$$\begin{cases} r_1^\alpha = r_{-1}^\alpha, & 0 \le x < \mathrm{x}_\alpha \\ r_1^\alpha + r_1^\beta = r_{-1}^\alpha + r_{-1}^\beta, & \mathrm{x}_\alpha \le x \le \mathrm{x}_\beta \\ r_1^\beta = r_{-1}^\beta, & \mathrm{x}_\beta < x \le 1 \end{cases} \tag{16}$$

Taking into account Bolzmann equation (Eq.4) and reaction rates (Eq.15) we can analytically solve Eq.16 and obtain general formula for equilibrium pressure:

$$P_{H_2}^{eq} = RT \begin{cases} \left(\dfrac{\theta}{1-\theta} \right)^2 \dfrac{k_{-1}^\alpha}{k_1^\alpha}, & 0 \le x < \mathrm{x}_\alpha \\ \dfrac{k_{-1}^\alpha (\theta_\alpha)^2 \mathrm{v}_\alpha + k_{-1}^\beta (\theta_\beta)^2 \mathrm{v}_\beta}{k_1^\alpha (1-\theta_\alpha)^2 \mathrm{v}_\alpha + k_1^\beta (1-\theta_\beta)^2 \mathrm{v}_\beta}, & \mathrm{x}_\alpha \le x \le \mathrm{x}_\beta \\ \left(\dfrac{\theta}{1-\theta} \right)^2 \dfrac{k_{-1}^\beta}{k_1^\beta}, & \mathrm{x}_\beta < x \le 1 \end{cases} \tag{17}$$

Note, that surface coverages θ, θ_i depend, in general, on state of charge. We find this dependence by considering second part of the reaction scheme. We also should remember that rate constants $k_1^\alpha, k_{-1}^\alpha, k_1^\beta, k_{-1}^\beta$ may be a functions of surface and bulk concentrations.

Part 2. Adsorption/absorption process is described by Eq.3 and shown in Fig.5. Phases at the surface and in the bulk of material (first atomic layer) are separated, so, reactions (Eq. 3) in both phases flow independently. Similar to Part 1 we can write adsorption (J_2^i) and desorption (J_{-2}^i) fluxes in phase i [mol/s] as

$$\begin{cases} J_2^i = \bar{k}_2^i \; A_i \; a_i^s(MH)\, a_i^b(M)\,, \\ J_{-2}^i = \bar{k}_{-2}^i \; A_i \; a_i^s(M)\, a_i^b(MH)\,, \end{cases} \quad i = \alpha, \beta \tag{18}$$

where $\bar{k}_2^i$, $i = \alpha, \beta$ [$m^3 mol^{-1} s^{-1}$] is the adsorption rate constant, $\bar{k}_{-2}^i$, $i = \alpha, \beta$ [$m^3 mol^{-1} s^{-1}$] is the desorption rate constant, $a_i^b(M)$ [mol m^{-2}] is the bulk activity (concentration) of free host sites in phase i, $a_i^b(MH)$ [mol m^{-2}] is the bulk activity (concentration) of occupied host sites in phase i. Denote a_0^b the density of available host sites in the bulk of the material (same for both phases). Then $a_0^b = a_i^b(M) + a_i^b(MH)$ and we may express bulk concentrations of occupied and freehost sites as

$$a_i^b(MH) = a_0^b \; x_i \quad \text{and} \qquad a_i^b(M) = a_0^b \; (1 - x_i) \quad i = \alpha, \beta\,.$$

Then for adsorption/desorption reaction rates [mol $s^{-1} m^{-2}$] we obtain

$$\begin{cases} r_2^i = k_2^i \; \theta_i (1 - x_i) \, \mathrm{v}_i\,, \quad i = \alpha, \beta \\ r_{-2}^i = k_{-2}^i \; x_i (1 - \theta_i) \, \mathrm{v}_i\,, \quad i = \alpha, \beta \end{cases} \tag{19}$$

where $k_1^i = \bar{k}_1^i a_0^s \, a_0^b$, $i = \alpha, \beta$ is the renormalized adsorption rate constant [mol $s^{-1} m^2$] and $k_{-1}^i = \bar{k}_{-1}^i \left[a_0^s \right]^2$, $i = \alpha, \beta$ is the renormalized recombination rate constant [mol $s^{-1} m^2$]. These constants are in fact depended on bulk and surface concentrations, but exact form of the dependencies will be given in the next section. Under the equilibrium conditions the rate of direct reaction is equal to the rate of the reverse reaction: $r_2^i = r_{-2}^i$ or

$$k_2^i \; \theta_i (1 - x_i) = k_{-2}^i \; x_i (1 - \theta_i)\,, i = \alpha, \beta \tag{20}$$

In general k_j^i may depend on state of charge and surface coverage. If exact form of this dependence is known then we can resolve Eq. 20 with respect to θ_i and obtain surface coverages. Let us observe, that k_j^i formally depends on material parameters such as a_0^s, a_0^b. However these parameters are unchanged during hydrogen storage process and may be treated just as normalization constants.

D. Rate constants description; “rectangle rule”

In case of hydrogen storage one has very complicated adsorption/absorption system. Dependence of the amount of adsorbed/adsorbed species on gas pressure under constant temperature is called adsorption/absorption isotherm.

The simplest isotherm has been proposed by Langmuir. According to his theory adsorbed atoms are situated in the same energy level and interaction between these atoms is ignored. Then in Langmuir theory surface coverage has the following simple explicit form[17,18,22]:

$$\theta = \frac{bP}{1+bP} \tag{21}$$

where P is pressure of adsorbing gas; $b = k_{ads} / k_{des}$ is the ratio of adsorption and desorption rate constants.

Generally accepted equation that expresses rate constant dependence on reaction temperature (T) and activation energy (E) is Arhenius equation[22]:

$$k = B\exp\left(-\frac{E}{kT}\right) \tag{22}$$

where B is predexponent frequency factor that characterizes probability of atomic collisions.

According to Langmuir theory rate constant described by Eq.21 is independent digital constant at certain temperature and it is not changed during chemical process. Thus, Langmuir theory is a good approximation if surface coverage is not so large. But for reactions with large surface coverages or absorption reactions where interaction forces are significant one can observe deviations from Langmuir theory.

The next step was semi-empirical theory of Temkin[23]. Temkin was taking into account experimentally observed fact that energy of adsorption is a linear function of surface coverage (with linear coefficient f). The final Temkin isotherm has form:

$$\theta = \frac{1}{f}\ln\left[\frac{1+bP}{1+bP\exp(-f)}\right] \tag{23}$$

where $b = k_{ads} / k_{des}$ is the ratio of adsorption and desorption rate constants. The other well-known isotherms (see e.g. Frumkin[24]) also have half-empirical basis and describe only limited number of chemical process.

So, if we try to describe some chemical reaction using above approaches we can determine that general kinetic equations (for example, for reaction rates) are the same but the difference is in rate constants definition. Thus, our conclusion is that the weakest point of above theories is that these theories don't give explicit and clear first principle description of the energy of the system and, as a result, equations for activation energies (and rate constants) in Eq.22 have completely empirical or half-empirical background.

In the present paper we give strong general energy description of the system and explicit algorithm of activation energies and rate constants derivation which can be applied not only in hydrogen storage system but to any considered reacting system.

Activation energy is an important characteristic of chemical process. It characterizes energy that one has to apply to the reacting atom to move it from one chemical stage (initial substances) to another stage (reaction products). Let us describe the energy levels of hydrogen storage process, consisting of adsorption/absorption (Eq.3) and recombination/dissosiation (Eq.2). The total energy diagram of the process is shown in the Fig.6. We can distinguish three areas in our system: bulk of the gas phase, surface layer and bulk of the hydride-forming material. To move one hydrogen atom from one area to another we have to apply to it certain activation energy to overcome the energy threshold (Π_{ij}). Activation energy is also one of the indications of the chemical reaction reversibility. If activation energy of direct reaction is smaller that that of reverse reaction, direct process is energetically more favorable.

Consider in more details the recombination process. Restrict derivation by considering separate phase i, ($i = \alpha, \beta$). Denote E_g^i the activation energy (per *molecule*) of the adsorption reaction and E_θ^i the activation energy (per *atom*) of the recombination reaction in given phase i. Accessing Fig.6 it is easy to see that E_g^i is the energy that hydrogen molecule needs to gain in order to reach the top of the potential barrier $\Pi_{g\theta}^i$ from the left, while for inverse reaction the energy gain of $2\mathrm{E}_\theta^i$ is necessary. If we denote

energy of one hydrogen molecule in the gas phase as ε_g (note that it is independent of phase), and energy of hydrogen atom in the surface layer as ε_θ^i then, by definition of potential barrier we have

$$\Pi_{g\theta}^i = 2(\mathrm{E}_\theta^i + \varepsilon_\theta^i) = \mathrm{E}_\theta^i + \varepsilon_g \tag{24}$$

Values of ε_θ^i can be regarded as marginal changes in the energies of the surface layer when amount of hydrogen atoms (n^s) is increased exactly by one. Similar ε_g is the marginal change in the internal energy of the gas phase when amount of molecules in is increased by one. The "rectangle rule" (Eq. 24) then gives us general tool to determine the rate constants from marginal energies, which are already well determined[13]. Thus we can write the individual rate constants:

$$\begin{cases} k_1^i = B_1^i \exp\left(-\dfrac{\mathrm{E}_g^i}{kT}\right) \\ k_{-1}^i = B_{-1}^i \exp\left(-\dfrac{2\mathrm{E}_\theta^i}{kT}\right) \end{cases} \Rightarrow \begin{cases} k_1^i = B_1^i \exp\left(-\dfrac{(\mathrm{E}_g^i + \varepsilon_g^i) - \varepsilon_g}{kT}\right) \\ k_{-1}^i = B_{-1}^i \exp\left(-\dfrac{2(\mathrm{E}_\theta^i + \varepsilon_\theta^i) - 2\varepsilon_\theta^i}{kT}\right) \end{cases} \Rightarrow \begin{cases} k_1^i = B_1^i \exp\left(-\dfrac{\Pi_{g\theta}^i}{kT}\right)\exp\left(\dfrac{\varepsilon_g}{kT}\right) \\ k_{-1}^i = B_{-1}^i \exp\left(-\dfrac{\Pi_{g\theta}}{kT}\right)\exp\left(\dfrac{2\varepsilon_\theta^i}{kT}\right) \end{cases} \tag{25}$$

In a similar way we consider absorption/desorbtion reaction. Denote $\overset{0}{\mathrm{E}}{}_\theta^i$ activation energy of the absorption reaction per hydrogen atom in phase i, E_x the activation energy of the desorbtion reaction per hydrogen atom and $\varepsilon_\theta^i, \varepsilon_x$ corresponding marginal energies. Then we obtain:

$$\Pi_{\theta x}^i = \overset{0}{\mathrm{E}}{}_\theta^i + \varepsilon_\theta^i = \mathrm{E}_x + \varepsilon_x, \tag{26}$$

where $\Pi_{\theta x}^i$ is the height of the potential barrier between surface and bulk. Then

$$\begin{cases} k_2^i = B_2^i \exp\left(-\dfrac{\overset{0}{\mathrm{E}}{}_\theta^i}{kT}\right) \\ k_{-2}^i = B_{-2}^i \exp\left(-\dfrac{\mathrm{E}_x}{kT}\right) \end{cases} \Rightarrow \begin{cases} k_2^i = B_2^i \exp\left(-\dfrac{(\overset{0}{\mathrm{E}}{}_\theta^i + \varepsilon_\theta^i) - \varepsilon_\theta^i}{kT}\right) \\ k_{-2}^i = B_{-2}^i \exp\left(-\dfrac{(\mathrm{E}_x + \varepsilon_x) - \varepsilon_x}{kT}\right) \end{cases} \Rightarrow \begin{cases} k_2^i = B_2^i \exp\left(-\dfrac{\Pi_{\theta x}^i}{kT}\right)\exp\left(\dfrac{\varepsilon_\theta^i}{kT}\right) \\ k_{-2}^i = B_{-2}^i \exp\left(-\dfrac{\Pi_{\theta x}^i}{kT}\right)\exp\left(\dfrac{\varepsilon_x}{kT}\right) \end{cases} \tag{27}$$

accordingly. The next section will explain derivation of the marginal energies ε_i-s.

E. System energy description

As follows from Eqs.25,27, in order to describe reaction rate constant we need to know the height of the potential barrier (Π_{ij}) and the marginal change in energy ε_i. To find the later value we have to know total energy of hydrogen atoms in any part of our system. Let us describe each part:

1. Bulk of the hydride-forming material.

The description of the energy of the bulk of hydride forming material is based on the application of the mean-field theory. General energy description follows from our LGM[13]. For convenience we reproduce general notions here.

To describe the energy of the hydrogen absorption system, a few aspects must be taken into account. First, the energy of the various host crystal lattices has to be considered. The contribution of each unit cell to the total energy is denoted as L_α and L_β for the α- and β-phase, respectively[25,26]. Secondly, the so-called Bragg-Williams approximation has been adopted, implying that the absorbed hydrogen atoms are randomly distributed in the hydride-forming material[27]. In the case of two-phase coexistence, two energetically different types of host sites coexist in the system and a binary alloy approach must be adopted. E_α^b and E_β^b represent the energy of absorbed hydrogen in both phases. It is, furthermore, assumed that an absorbed hydrogen atom at a particular site can interact with a hydrogen atom at any other site[2], with specific interaction energy (U_{ii}^b). According to the mean-field approximation[27] the interaction energy between the occupied sites does not depend on their distance. $U_{\alpha\alpha}^b$ and $U_{\beta\beta}^b$ are the interaction energies between two absorbed atoms in the α- and β-phase, respectively, and $U_{\alpha\beta}^b$ represents the interaction energy between two absorbed hydrogen atoms in different phases[27]. These considerations lead to the following Hamiltonian (U^b) for the entire bulk of the hydrogen storage system:

$$U^b = L_\alpha M_\alpha + L_\beta M_\beta + E_\alpha^b n_\alpha^b + E_\beta^b n_\beta^b + \frac{U_{\alpha\alpha}^b}{2n_{\max}^b}(n_\alpha^b)^2 + \frac{U_{\beta\beta}^b}{2n_{\max}^b}(n_\beta^b)^2 + \frac{U_{\alpha\beta}^b}{2n_{\max}^b} n_\alpha^b n_\beta^b \qquad (28)$$

Taking into account definition of M_α^b and M_β^b in Eq.5, the first two terms in Eq.28 can be rewritten as

$$L_\alpha M_\alpha^b + L_\beta M_\beta^b = L_\alpha M^b + (L_\beta - L_\alpha) M_\beta^b = L_\alpha M^b + \frac{(L_\beta - L_\alpha) n_{\max}^b}{d^b} \quad . \tag{29}$$

where d^b is the number of host sites per bulk unit cell.

We assumed the same number of host sites per unit cell for both phases ($d^b = 1$). Replacing n_α^b and n_β^b by x using Eq.7, the following relationships are obtained for the three considered crystallographic regions:

$$U^b = n_{\max}^b \begin{cases} \dfrac{L_\alpha M^b}{n_{\max}^b} + E_\alpha^b x + \dfrac{U_{\alpha\alpha}^b}{2} x^2, & x < \mathrm{x}_\alpha \\ L_\alpha + (L_\beta - L_\alpha)\mathrm{v}_\beta + E_\alpha^b \mathrm{x}_\alpha \mathrm{v}_\alpha + E_\beta^b \mathrm{x}_\beta \mathrm{v}_\beta + \dfrac{U_{\alpha\alpha}^b \mathrm{x}_\alpha^2}{2} \mathrm{v}_\alpha^2 + & \\ \dfrac{U_{\beta\beta}^b \mathrm{x}_\beta^2}{2} \mathrm{v}_\beta^2 + \dfrac{U_{\alpha\beta}^b \mathrm{x}_\alpha \mathrm{x}_\beta}{2} \mathrm{v}_\alpha \mathrm{v}_\beta, & \mathrm{x}_\alpha \le x \le \mathrm{x}_\beta \\ \dfrac{L_\beta M^b}{n_{\max}^b} + E_\beta^b x + \dfrac{U_{\beta\beta}^b}{2} x^2, & x > \mathrm{x}_\beta \end{cases} . \tag{30}$$

As we noted above, ε_x is a marginal change in the energy of bulk when amounts of hydrogen atoms n^b is increased exactly by one. Since $n^b = x n_{\max}^b$, it follows that $\frac{\partial U^b}{\partial n^b} \Delta n^b = \frac{\partial U^b}{\partial n^b} \cdot 1 = \frac{1}{n_{\max}^b} \frac{\partial U^b}{\partial x}$ up to higher order term with respect to $1/n_{\max}^b$. Then differentiating Eq.30 with respect to x ultimately leads to:

$$\varepsilon_x = \frac{1}{n_{\max}^b} \frac{\partial U^b}{\partial x} = \begin{cases} E_\alpha^b + U_{\alpha\alpha}^b x, & x < \mathrm{x}_\alpha \\ \dfrac{E_\beta^b \mathrm{x}_\beta - E_\alpha^b \mathrm{x}_\alpha - U_{\alpha\alpha}^b \mathrm{x}_\alpha^2 \mathrm{v}_\alpha + U_{\alpha\beta}^b \mathrm{x}_\beta^2 \mathrm{v}_\beta + U_{\beta\beta}^b \mathrm{x}_\alpha \mathrm{x}_\beta (\mathrm{v}_\alpha - \mathrm{v}_\beta)/2 + L}{\mathrm{x}_\beta - \mathrm{x}_\alpha}, & \\ & \mathrm{x}_\alpha \le x \le \mathrm{x}_\beta \\ E_\beta^b + U_{\beta\beta}^b x, & x > \mathrm{x}_\beta \end{cases} \tag{31}$$

where $L = L_\beta - L_\alpha$.

Apparently there is no difference to which phase hydrogen atom goes during absorption, or from which phase it had gone during desorption, thus we have only ε_x but not two separate ε_x^α and ε_x^β. The intuition behind this phenomenon is simple. Suppose that bulk of the material contain both phases. Then, irrelevant where we put additional hydrogen atoms in the bulk, the amount of α-phase will decrease while amount of β-phase will increase.[1] Therefore marginal change in energy of the bulk does not depend on phase where additional hydrogen atom was inserted. In mathematical terms it states that variables n_α^b and n_β^b are not independent variables in the two-phase coexistence region.

2. Surface hydride-forming material.

To describe the energy of the hydrogen adsorption system we applied similar mean-field conception as for the bulk. These considerations lead us to the following Hamiltonian (U^s) for the hydrogen adsorbed in the surface of the hydride-forming material:

$$U^s = E_\alpha^s n_\alpha^s + E_\beta^s n_\beta^s + \frac{U_{\alpha\alpha}^s (n_\alpha^s)^2}{2n_{\max}^s} + \frac{U_{\beta\beta}^s (n_\beta^s)^2}{2n_{\max}^s} + \frac{U_{\alpha\beta}^s n_\alpha^s n_\beta^s}{2n_{\max}^s} \qquad (32)$$

where E_i^s are energies of one separate hydrogen atom adsorbed in the phase *i* of the surface of the hydride-forming material; U_{ii}^s are interaction energies between adsorbed hydrogen atoms in phase *i*; $U_{\alpha\beta}^s$ is interaction energy between adsorbed hydrogen atoms in different phases; n_i^s is the number of atoms adsorbed in the phase *i*; $i = \alpha, \beta$.

Hamiltonian (U^s) in Eq.32 is different from the bulk Hamiltonian (U^b) described in Eq.28. First two terms, associated with the crystal lattice are absent, since there is no lattice at the surface. Another important fact about surface Hamiltonian is that variables n_α^s and n_β^s are independent, contrary to situation with n_α^b and n_β^b. Indeed, hydrogen atoms can leave surface layer from α-phase region, and it does have absolutely no influence onto the β-phase, since maximal capacities of surface phases are determined by

[1] Remember, that concentrations of hydrogen atoms inside pure phase remain constant (and equal to x_α or x_β correspondingly) during phase transition process.

bulk concentrations, not by surface ones[2]. Now consider the marginal changes in the energy of surface layer when amounts of hydrogen atoms n_α^s and n_β^s are increased exactly by one, that is:

$$\begin{cases} \varepsilon_\theta^\alpha = \dfrac{\partial U^s}{\partial n_\alpha^s} = E_\alpha^s + U_{\alpha\alpha}^s \dfrac{n_\alpha^s}{n_{\max}^s} + U_{\alpha\beta}^s \dfrac{n_\beta^s}{n_{\max}^s} = E_\alpha^s + U_{\alpha\alpha}^s \theta^\alpha + U_{\alpha\beta}^s \theta^\beta / 2 \\ \varepsilon_\theta^\beta = \dfrac{\partial U^s}{\partial n_\beta^s} = E_\beta^s + U_{\beta\beta}^s \dfrac{n_\beta^s}{n_{\max}^s} + U_{\alpha\beta}^s \dfrac{n_\alpha^s}{n_{\max}^s} = E_\beta^s + U_{\beta\beta}^s \theta^\beta + U_{\alpha\beta}^s \theta^\alpha / 2 \end{cases} \tag{33}$$

Note, that difference $\varepsilon_x - \varepsilon_\theta^i$ is well interpreted according to

$$\varepsilon_x - \varepsilon_\theta^i = \frac{\partial U^b}{\partial n^b} \times (+1) + \frac{\partial U^s}{\partial n_i^s} \times (-1) = \frac{\partial U^b}{\partial n^b} \Delta n^b + \frac{\partial U^s}{\partial n_i^s} \Delta n_i^s = \Delta_i (U^b + U^s), \tag{34}$$

where the last right hand term corresponds to the change in the energy of the (closed) system: surface + bulk when exactly one hydrogen atom moves in the i-th phase from the surface layer into the bulk according to the positive direction of absorption reaction.

3. Hydrogen in the gas phase.

To describe the energy of hydrogen in the gas phase we applied similar mean-field conception as for adsorption/absorption state. These considerations lead us to the following very simple Hamiltonian (U^g) for the hydrogen in the gas phase:

$$U^g = E^g n^g \tag{35}$$

where E^g is the energy of one separate hydrogen atom; n^g is the number of hydrogen atoms dissolved in the bulk of the gas phase.

Differentiating of Eq.35 with respect to n^g ultimately leads us to:

[2] Strictly speaking this statement is only approximately correct, because the *same* hydrogen atom can enter the bulk and therefore change somewhat phase distributions. This change of phase distributions, in turn will change surface phase areas and it will change the number of hydrogen atoms in each of these areas, consequently changing the value of Hamiltonian. However this effect is negligibly small if $n_{\max}$ is sufficiently large.

$$\varepsilon_g = \frac{\partial U^g}{\partial n^g} = E^g \tag{36}$$

The handbook theories[28] for internal energy of two-atomic ideal gas give us $E^g = 5kT/2$, thus

$$\varepsilon_g = \frac{5}{2}kT \tag{37}$$

F. Final equations

Substituting Eq.31,33 into Eq.27 we obtain expressions for the adsorption/absorption rate constants:

$$\begin{aligned}
&k_2^i = B_2^i \exp\left(-\frac{\Pi_{\theta x}^i}{kT}\right)\exp\left(\frac{E_i^s + U_{ii}^s\theta^i + U_{\alpha\beta}^s\theta^j/2}{(kT/e)}\right), i,j = \alpha,\beta; i \neq j.\\
&k_{-2}^\alpha = B_{-2}^\alpha \exp\left(-\frac{\Pi_{\theta x}^\alpha}{kT}\right)\begin{cases}\exp\left(\dfrac{E_\alpha^b + U_{\alpha\alpha}^b x}{(kT/e)}\right), & x < \mathrm{x}_\alpha,\\ \exp\left(\dfrac{E_\beta^b \mathrm{x}_\beta - E_\alpha^b \mathrm{x}_\alpha - U_{\alpha\alpha}^b \mathrm{x}_\alpha^2 \mathrm{v}_\alpha + U_{\beta\beta}^b \mathrm{x}_\beta^2 \mathrm{v}_\beta + U_{\alpha\beta}^b \mathrm{x}_\alpha \mathrm{x}_\beta(\mathrm{v}_\alpha - \mathrm{v}_\beta)/2 + L}{(kT/e)(\mathrm{x}_\beta - \mathrm{x}_\alpha)}\right), & \mathrm{x}_\alpha \le x \le \mathrm{x}_\beta,\end{cases}\\
&k_{-2}^\beta = B_{-2}^\beta \exp\left(-\frac{\Pi_{\theta x}^\beta}{kT}\right)\begin{cases}\exp\left(\dfrac{E_\beta^b \mathrm{x}_\beta - E_\alpha^b \mathrm{x}_\alpha - U_{\alpha\alpha}^b \mathrm{x}_\alpha^2 \mathrm{v}_\alpha + U_{\beta\beta}^b \mathrm{x}_\beta^2 \mathrm{v}_\beta + U_{\alpha\beta}^b \mathrm{x}_\alpha \mathrm{x}_\beta(\mathrm{v}_\alpha - \mathrm{v}_\beta)/2 + L}{(kT/e)(\mathrm{x}_\beta - \mathrm{x}_\alpha)}\right), & \mathrm{x}_\alpha \le x \le \mathrm{x}_\beta,\\ \exp\left(\dfrac{E_\beta^b + U_{\beta\beta}^b x}{(kT/e)}\right), & x > \mathrm{x}_\beta.\end{cases}
\end{aligned} \tag{38}$$

Substituting Eq.38 into Eqs.19,20 we obtain following set of equations for the surface coverage in three considered crystallographic regions:

$$\begin{cases}
\dfrac{x(1-\theta)}{\theta(1-x)} = \dfrac{B_2^\alpha}{B_{-2}^\alpha}\exp\left(\dfrac{E_\alpha^s + U_{\alpha\alpha}^s\theta - (E_\alpha^b + U_{\alpha\alpha}^b x)}{(RT/F)}\right), & 0 \le x < \mathrm{x}_\alpha\\
\dfrac{x_i(1-\theta_i)}{\theta_i(1-x_i)} = & \\
\dfrac{B_2^i}{B_{-2}^i}\exp\left(\dfrac{E_i^s + U_{ii}^s\theta^i + U_{\alpha\beta}^s\theta^j/2}{(RT/F)} - \dfrac{E_\beta^b \mathrm{x}_\beta - E_\alpha^b \mathrm{x}_\alpha - U_{\alpha\alpha}^b \mathrm{x}_\alpha^2 \mathrm{v}_\alpha + U_{\beta\beta}^b \mathrm{x}_\beta^2 \mathrm{v}_\beta + U_{\alpha\beta}^b \mathrm{x}_\alpha \mathrm{x}_\beta(\mathrm{v}_\alpha - \mathrm{v}_\beta)/2 + L}{(RT/F)(\mathrm{x}_\beta - \mathrm{x}_\alpha)}\right). & \\
\qquad \mathrm{x}_\alpha \le x \le \mathrm{x}_\beta; i,j = \alpha,\beta; i \neq j, & \\
\dfrac{x(1-\theta)}{\theta(1-x)} = \dfrac{B_2^\beta}{B_{-2}^\beta}\exp\left(\dfrac{E_\beta^s + U_{\beta\beta}^s\theta - (E_\beta^b + U_{\beta\beta}^b x)}{(RT/F)}\right), & \mathrm{x}_\beta < x \le 1
\end{cases} \tag{39}$$

Note that additional parameters $\Pi^{\alpha}_{\theta x}$ and $\Pi^{\beta}_{\theta x}$ can be reduced in equilibrium equation. The set of Eq.39 is a complex highly nonlinear two-dimensional system with two unknowns and its analytical solution is impossible. To calculate total and partial surface coverages we have to solve it numerically. But the complexity of solution anyway remains very high. In order to reduce complexity of the system we applied consequently simplifying assumption that there are no inter-phase interactions in the surface layer, i.e.

$$U^{s}_{\alpha\beta} = 0\,. \tag{40}$$

Simplification Eq.40 also has physical background. In the surface layer, in general, interaction energy between adsorbed atoms is smaller than in the absorbed state. The reasons are absence of influence of the crystallographic structure and bigger distance between adsorbed atoms: closed unit cell in the bulk of the material is, apparently a tighter system than half open unit cell at the surface. Thus, we may apply condition Eq.40 to simplify mathematics. By the same reason we expect that values of interaction energies at the surface ($U^{s}_{\alpha\alpha}$ and $U^{s}_{\beta\beta}$) are several orders smaller than those in the bulk ($U^{b}_{\alpha\alpha}$ and $U^{b}_{\beta\beta}$).

After applying Eq. 40 the system of equations (Eq.39) can be separated into two one-dimensional equations. One is for surface coverage in the α-phase,

$$\frac{x(1-\theta)}{\theta(1-x)} = \frac{B^{\alpha}_{2}}{B^{\alpha}_{-2}}\exp\left(\frac{E^{s}_{\alpha}+U^{s}_{\alpha\alpha}\theta-(E^{b}_{\alpha}+U^{b}_{\alpha\alpha}x)}{(RT/F)}\right), \qquad 0 \le x < \mathrm{x}_{\alpha}, \tag{41a}$$

$$\frac{x_i(1-\theta_i)}{\theta_i(1-x_i)} = \frac{B^{\alpha}_{2}}{B^{\alpha}_{-2}}\exp\left(\frac{E^{s}_{\alpha}+U^{s}_{\alpha\alpha}\theta^{\alpha}}{(RT/F)} - \frac{E^{b}_{\beta}\mathrm{x}_{\beta}-E^{b}_{\alpha}\mathrm{x}_{\alpha}-U^{b}_{\alpha\alpha}\mathrm{x}^{2}_{\alpha}\mathrm{v}_{\alpha}+U^{b}_{\beta\beta}\mathrm{x}^{2}_{\beta}\mathrm{v}_{\beta}+U^{b}_{\alpha\beta}\mathrm{x}_{\alpha}\mathrm{x}_{\beta}(\mathrm{v}_{\alpha}-\mathrm{v}_{\beta})/2+L}{(RT/F)(\mathrm{x}_{\beta}-\mathrm{x}_{\alpha})}\right),$$

$$\text{when} \quad \mathrm{x}_{\alpha} \le x \le \mathrm{x}_{\beta}$$

another is for surface coverage in β phase

$$\frac{x_i(1-\theta_i)}{\theta_i(1-x_i)}=\frac{B_2^\beta}{B_{-2}^\beta}\exp\left(\frac{E_\beta^s+U_{\beta\beta}^s\theta^\beta}{(RT/F)}-\frac{E_\beta^b\mathrm{x}_\beta-E_\alpha^b\mathrm{x}_\alpha-U_{\alpha\alpha}^b\mathrm{x}_\alpha^2\mathrm{v}_\alpha+U_{\beta\beta}^b\mathrm{x}_\beta^2\mathrm{v}_\beta+U_{\alpha\beta}^b\mathrm{x}_\alpha\mathrm{x}_\beta(\mathrm{v}_\alpha-\mathrm{v}_\beta)/2+L}{(RT/F)(\mathrm{x}_\beta-\mathrm{x}_\alpha)}\right),$$

when $\mathrm{x}_\alpha \le x \le \mathrm{x}_\beta$

$$\frac{x(1-\theta)}{\theta(1-x)}=\frac{B_2^\beta}{B_{-2}^\beta}\exp\left(\frac{E_\beta^s+U_{\beta\beta}^s\theta-(E_\beta^b+U_{\beta\beta}^b x)}{(RT/F)}\right),\qquad \mathrm{x}_\beta < x \le 1. \qquad (41b)$$

Eqs.41(a-b) can be solved numerically for each value of x, providing functions $\theta(x)$, $\theta^i(x)$, $\theta_i(x)$. Substituting Eqs.33,37 into Eq.25 and taking into account simplification Eq.40 we obtained expressions for the dissociation/recombination rate constants:

$$k_1^i=B_1^i\exp\left(-\frac{\Pi_{g\theta}^i}{kT}\right)\exp\left(\frac{5}{2}\right),$$

$$i=\alpha,\beta \qquad (42)$$

$$k_{-1}^i=B_{-1}^i\exp\left(-\frac{\Pi_{g\theta}^i}{kT}\right)\exp\left(2\frac{E_i^s+U_{ii}^s\theta^i}{(kT/e)}\right)$$

Substituting Eqs.42 into Eq.18 we obtain the final expression for the equilibrium hydrogen pressure

$$P_{H_2}^{eq}=RT\begin{cases}\left(\dfrac{\theta}{1-\theta}\right)^2\dfrac{B_{-1}^\alpha}{B_1^\alpha}\exp\left(2\dfrac{E_\alpha^s+U_{\alpha\alpha}^s\theta}{(RT/F)}\right)\exp(-5/2), & 0\le x<\mathrm{x}_\alpha\\ \dfrac{\left[B_{-1}^\alpha\exp\left(2\dfrac{E_\alpha^s+U_{\alpha\alpha}^s\theta^\alpha}{(RT/F)}\right)(\theta_\alpha)^2\mathrm{v}_\alpha+B_{-1}^\beta\exp\left(\dfrac{\Delta\Pi}{kT}\right)\exp\left(2\dfrac{E_\beta^s+U_{\beta\beta}^s\theta^\beta}{(RT/F)}\right)(\theta_\beta)^2\mathrm{v}_\beta\right]}{\left[B_1^\alpha(1-\theta_\alpha)^2\mathrm{v}_\alpha+B_1^\beta\exp\left(\dfrac{\Delta\Pi}{kT}\right)(1-\theta_\beta)^2\mathrm{v}_\beta\right]\exp(5/2)}, & \mathrm{x}_\alpha\le x\le\mathrm{x}_\beta\\ \left(\dfrac{\theta}{1-\theta}\right)^2\dfrac{B_{-1}^\beta}{B_1^\beta}\exp\left(2\dfrac{E_\beta^s+U_{\beta\beta}^s\theta}{(RT/F)}\right)\exp(-5/2), & \mathrm{x}_\beta<x\le1\end{cases} \qquad (43)$$

where $\Delta\Pi=\Pi_{g\theta}^\alpha-\Pi_{g\theta}^\beta$.

G. Identification and simplifications. General remarks.

Eqs.41(a-b) and Eq.43 let us simulate the hydrogen pressure composition isotherm. We, however, can observe that sometimes different parameter values still lead to the same surface coverage and equilibrium pressure. For example only the ratio of parameters $B_2^\alpha / B_{-2}^\alpha$ enters Eq.41a, but not each of these parameters separately. Therefore only the ratio $B_2^\alpha / B_{-2}^\alpha$ can be identified from experimental data, but not B_2^α and B_{-2}^α separately. To remove that source of identification problem we denote:

$$\mathrm{B}_1^\alpha = B_{-1}^\alpha / B_1^\alpha ,\ \ \mathrm{B}_1^\beta = B_{-1}^\beta / B_1^\beta ,\ \ B_1^{\alpha\beta} = B_1^\alpha / B_1^\beta ,\ B_2^\alpha = B_2^\alpha / B_{-2}^\alpha ,\ \ \mathrm{B}_2^\beta = B_2^\beta / B_{-2}^\beta . \qquad (44)$$

Equations (41) then reduces to

$$\frac{x(1-\theta)}{\theta(1-x)} = \mathrm{B}_2^\alpha \exp\left(\frac{E_\alpha^s + U_{\alpha\alpha}^s \theta - (E_\alpha^b + U_{\alpha\alpha}^b x)}{(RT/F)} \right), \qquad 0 \le x < \mathrm{x}_\alpha , \qquad (45a)$$

$$\frac{x_i(1-\theta_i)}{\theta_i(1-x_i)} = \mathrm{B}_2^\alpha \exp\left(\frac{E_\alpha^s + U_{\alpha\alpha}^s \theta^\alpha}{(RT/F)} - \frac{E_\beta^b \mathrm{x}_\beta - E_\alpha^b \mathrm{x}_\alpha - U_{\alpha\alpha}^b \mathrm{x}_\alpha^2 \mathrm{v}_\alpha + U_{\beta\beta}^b \mathrm{x}_\beta^2 \mathrm{v}_\beta + U_{\alpha\beta}^b \mathrm{x}_\alpha \mathrm{x}_\beta (\mathrm{v}_\beta - \mathrm{v}_\alpha)/2 + L}{(RT/F)(\mathrm{x}_\beta - \mathrm{x}_\alpha)} \right), \mathrm{x}_\alpha \le x \le \mathrm{x}_\beta$$

and

$$\frac{x_i(1-\theta_i)}{\theta_i(1-x_i)} = \mathrm{B}_2^\beta \exp\left(\frac{E_\beta^s + U_{\beta\beta}^s \theta^\beta}{(RT/F)} - \frac{E_\beta^b \mathrm{x}_\beta - E_\alpha^b \mathrm{x}_\alpha - U_{\alpha\alpha}^b \mathrm{x}_\alpha^2 \mathrm{v}_\alpha + U_{\beta\beta}^b \mathrm{x}_\beta^2 \mathrm{v}_\beta + U_{\alpha\beta}^b \mathrm{x}_\alpha \mathrm{x}_\beta (\mathrm{v}_\alpha - \mathrm{v}_\beta)/2 + L}{(RT/F)(\mathrm{x}_\beta - \mathrm{x}_\alpha)} \right), \mathrm{x}_\alpha \le x \le \mathrm{x}_\beta ,$$

$$\frac{x(1-\theta)}{\theta(1-x)} = \mathrm{B}_2^\beta \exp\left(\frac{E_\beta^s + U_{\beta\beta}^s \theta - (E_\beta^b + U_{\beta\beta}^b x)}{(RT/F)} \right), \qquad \mathrm{x}_\beta < x \le 1. \qquad (45b)$$

accordingly.

In similar way we may simplify equation Eq.43. However there we have put one more simplifying restriction namely $\Delta\Pi = 0$. The physical sense behind this restriction is the following. We expect that influence of the bulk phase declines when we moving far away from the hydride-forming material. This influence is absent in the bulk of the gas phase and therefore must be extremely week just outside the surface layer. Therefore we expect that height of the potential barrier for dissociation reaction doesn't depend on phase. Again note, that $\Pi_{g\theta}^\alpha$ and $\Pi_{g\theta}^\beta$ may, in general, be functions of state of charge and surface coverage(s). We require only $\Delta\Pi = \Pi_{g\theta}^\alpha - \Pi_{g\theta}^\beta = 0$ i.e. those barriers are same in both phases. Thus we obtain:

$$P_{H_2}^{eq} = RT\begin{cases}\left(\dfrac{\theta}{1-\theta}\right)^2 \mathrm{B}_1^{\alpha}\exp\left(2\dfrac{E_\alpha^s + U_{\alpha\alpha}^s\theta}{(RT/F)}\right)\exp(-5/2), & 0 \le x < \mathrm{x}_\alpha, \\ \dfrac{\left[\mathrm{B}_1^{\alpha}\mathrm{B}_1^{\alpha\beta}\exp\left(2\dfrac{E_\alpha^s + U_{\alpha\alpha}^s\theta^\alpha}{(RT/F)}\right)(\theta_\alpha)^2\mathrm{v}_\alpha + \mathrm{B}_1^{\beta}\exp\left(2\dfrac{E_\beta^s + U_{\beta\beta}^s\theta^\beta}{(RT/F)}\right)(\theta_\beta)^2\mathrm{v}_\beta\right]}{\left[\mathrm{B}_1^{\alpha\beta}(1-\theta_\alpha)^2\mathrm{v}_\alpha + (1-\theta_\beta)^2\mathrm{v}_\beta\right]\exp(5/2)}, & \mathrm{x}_\alpha \le x \le \mathrm{x}_\beta, \\ \left(\dfrac{\theta}{1-\theta}\right)^2 \mathrm{B}_1^{\beta}\exp\left(2\dfrac{E_\beta^s + U_{\beta\beta}^s\theta}{(RT/F)}\right)\exp(-5/2), & \mathrm{x}_\beta < x \le 1. \end{cases} \quad (46)$$

Eq.46 was derived from the equilibrium rate balance conditions Eqs.17, which represents equality of the rates for direct and reverse reactions. It is of interest, therefore, to obtain expressions for the rates of dissociation and recombination[3] as functions of parameters of the system and state variables:

$$r_1 = \exp\left(\frac{5}{2}\right)a_g\begin{cases}(1-\theta)^2, & 0 \le x < x_\alpha, \\ \mathrm{B}_1^{\alpha\beta}\mathrm{B}_1^{\alpha\beta}(1-\theta_\alpha)^2\mathrm{v}_\alpha + (1-\theta_\beta)^2\mathrm{v}_\beta, & x_\alpha \le x \le x_\beta, \\ (1-\theta)^2, & x_\beta < x \le 1. \end{cases} \quad (47)$$

$$r_{-1} = \begin{cases}\mathrm{B}_1^{\alpha}\theta^2\exp\left(2\dfrac{E_\alpha^s + U_{\alpha\alpha}^s\theta}{(RT/F)}\right), & 0 \le x < \mathrm{x}_\alpha \\ \mathrm{B}_1^{\alpha}\mathrm{B}_1^{\alpha\beta}\exp\left(2\dfrac{E_\alpha^s + U_{\alpha\alpha}^s\theta^\alpha}{(RT/F)}\right)(\theta_\alpha)^2\mathrm{v}_\alpha + \mathrm{B}_1^{\beta}\exp\left(2\dfrac{E_\beta^s + U_{\beta\beta}^s\theta^\beta}{(RT/F)}\right)(\theta_\beta)^2\mathrm{v}_\beta, & \mathrm{x}_\alpha \le x \le \mathrm{x}_\beta \\ \mathrm{B}_1^{\beta}\theta^2\exp\left(2\dfrac{E_\beta^s + U_{\beta\beta}^s\theta}{(RT/F)}\right), & \mathrm{x}_\beta < x \le 1 \end{cases}. \quad (48)$$

Note, that Eq.47,48 are, in general, discontinuous at the point of first phase transition, that is for values of θ corresponding x_α. However physical sense requires that r_1 and r_{-1} have to be continuous. To maintain continuity at the point of phase transition it is sufficient to impose the following condition:

$$\mathrm{B}_1^{\alpha\beta} = 1 \quad (49)$$

[3] We normalized all rates setting corresponding Π_{jk}^i to zero. It also applies to absorption/desorption rates.

Finally, using Eqs.45(a,b) and reaction rate balance equations Eqs.19,20 we can write rates of direct and reverse reactions of adsorption/absorption process which are also useful for simulation:

$$r_2 = \begin{cases} \mathrm{B}_2^{\alpha} \exp\left(\dfrac{E_{\alpha}^{s} + U_{\alpha\alpha}^{s}\theta}{(RT/F)} \right) \theta(1-x), & 0 \le x < \mathrm{x}_{\alpha}, \\ \mathrm{B}_2^{\alpha} \exp\left(2\dfrac{E_{\alpha}^{s} + U_{\alpha\alpha}^{s}\theta^{\alpha}}{(RT/F)} \right) \theta_{\alpha}(1-x_{\alpha})\mathrm{v}_{\alpha} + \mathrm{B}_2^{\beta} \exp\left(2\dfrac{E_{\beta}^{s} + U_{\beta\beta}^{s}\theta^{\beta}}{(RT/F)} \right) \theta_{\beta}(1-x_{\beta})\mathrm{v}_{\beta}, & \\ & \mathrm{x}_{\alpha} \le x \le \mathrm{x}_{\beta}, \\ \mathrm{B}_2^{\beta} \exp\left(2\dfrac{E_{\beta}^{s} + U_{\beta\beta}^{s}\theta}{(RT/F)} \right) \theta(1-x), & \mathrm{x}_{\beta} < x \le 1. \end{cases} \tag{50}$$

$$r_{-2} = \begin{cases} \exp\left(\dfrac{E_{\alpha}^{b} + U_{\alpha\alpha}^{b}x}{(RT/F)} \right) x(1-\theta), & 0 \le x < \mathrm{x}_{\alpha} \\ \exp\left(\dfrac{E_{\beta}^{b}\mathrm{x}_{\beta} - E_{\alpha}^{b}\mathrm{x}_{\alpha} - U_{\alpha\alpha}^{b}\mathrm{x}_{\alpha}^{2}\mathrm{v}_{\alpha} + U_{\beta\beta}^{b}\mathrm{x}_{\beta}^{2}\mathrm{v}_{\beta} + U_{\alpha\beta}^{b}\mathrm{x}_{\alpha}\mathrm{x}_{\beta}(\mathrm{v}_{\alpha} - \mathrm{v}_{\beta})/2 + L}{(RT/F)(\mathrm{x}_{\beta} - \mathrm{x}_{\alpha})} \right) \times & \\ \left((1-\theta_{\alpha})x_{\alpha}\mathrm{v}_{\alpha} + (1-\theta_{\beta})x_{\beta}\mathrm{v}_{\beta} \right), & \mathrm{x}_{\alpha} \le x \le \mathrm{x}_{\beta} \\ \exp\left(\dfrac{E_{\beta}^{b} + U_{\beta\beta}^{b}x}{(RT/F)} \right) x(1-\theta), & \mathrm{x}_{\beta} < x \le 1 \end{cases} . \tag{51}$$

H. Connection with the Lattice Gas Model.

In the previous paper we presented pure statistical thermodynamic Lattice Gas Model[13]. The total energy of hydrogen storage system has been described by energy Hamiltonian Eq.28. The model defines the pressure as explicit functions of the normalized hydrogen concentration x with eight parameters, *i.e.* the phase-transition points (x_{α} and x_{β}), the energies of individual hydrogen atoms (E_{α} and E_{β}), the interaction energies within the α and β phases ($U_{\alpha\alpha}$ and $U_{\beta\beta}$), the interaction energy between hydrogen atoms in the different phases ($U_{\alpha\beta}$), and the energy of the crystal structure (host energy, L). In the Lattice Gas Model[13] the equilibrium hydrogen pressure is determined as:

$$P_{H_2} = P_{ref} \exp\begin{cases} \dfrac{2e\left(E_\alpha + U_{\alpha\alpha}x\right)}{kT} - 2\ln\left(\dfrac{1-xd}{xd}\right), & 0 \le x < \mathrm{x}_\alpha \\ \dfrac{2e}{kT}\left\{-E_\alpha \mathrm{x}_\alpha - U_{\alpha\alpha}\mathrm{x}_\alpha^2 x_2 + E_\beta \mathrm{x}_\beta + U_{\beta\beta}\mathrm{x}_\beta^2 x_1 + \dfrac{U_{\alpha\beta}\mathrm{x}_\alpha \mathrm{x}_\beta}{2}(x_2 - x_1) + L\right\} - 2\left(\dfrac{S_\alpha^0}{d} - S_\beta^0\right) \\ \hline (\mathrm{x}_\beta - \mathrm{x}_\alpha) \\ \mathrm{x}_\alpha \le x \le \mathrm{x}_\beta \\ \dfrac{2e\left(E_\beta + U_{\beta\beta}x\right)}{kT} - 2\ln\left(\dfrac{1-x}{x}\right), & \mathrm{x}_\beta < x \le 1 \end{cases} \quad (52)$$

where, in fact $x_1 = \mathrm{v}_\beta$ and $x_2 = \mathrm{v}_\alpha$ and entropy terms are the follows:

$$S_\alpha^0 = \mathrm{x}_\alpha d \ln \mathrm{x}_\alpha d + (1 - \mathrm{x}_\alpha d)\ln(1 - \mathrm{x}_\alpha d)$$
$$S_\beta^0 = \mathrm{x}_\beta \ln \mathrm{x}_\beta + (1 - \mathrm{x}_\beta)\ln(1 - \mathrm{x}_\beta)\,. \quad (53)$$

with the following continuity conditions:

$$L = D_{\alpha\beta} - E_\beta \mathrm{x}_\beta + E_\alpha \mathrm{x}_\alpha + \frac{U_{\alpha\alpha}\mathrm{x}_\alpha^2 - U_{\beta\beta}\mathrm{x}_\beta^2}{2} - \left\{D_\alpha + D_\beta - (E_\alpha + E_\beta) - (U_{\alpha\alpha}\mathrm{x}_\alpha + U_{\beta\beta}\mathrm{x}_\beta)\right\}\frac{(\mathrm{x}_\beta - \mathrm{x}_\alpha)}{2},$$

$$U_{\alpha\beta} = \frac{U_\alpha \mathrm{x}_\alpha^2 + U_{\beta\beta}\mathrm{x}_\beta^2}{\mathrm{x}_\alpha \mathrm{x}_\beta} - \frac{D_\alpha - D_\beta - E_\alpha + E_\beta - U_{\alpha\alpha}\mathrm{x}_\alpha + U_{\beta\beta}\mathrm{x}_\beta}{\mathrm{x}_\alpha \mathrm{x}_\beta}(\mathrm{x}_\beta - \mathrm{x}_\alpha). \quad (54)$$

where

$$D_\alpha = \frac{kT}{e}\ln\left(\frac{1 - \mathrm{x}_\alpha d}{\mathrm{x}_\alpha d}\right),\ D_\beta = \frac{kT}{e}\ln\left(\frac{1 - \mathrm{x}_\beta}{\mathrm{x}_\beta}\right),\ D_{\alpha\beta} = \frac{kT}{e}\left(\frac{S_\alpha^0}{d} - S_\beta^0\right). \quad (55)$$

Note that restriction $d = 1$ was used in all simulations. Obviously the phase-transition points (x_α and x_β) in both Lattice Gas Model and Kinetic Model are the same. Correspondence between the energies of individual hydrogen atoms (E_α and E_β), the interaction energies within the α and β phases ($U_{\alpha\alpha}$ and $U_{\beta\beta}$) in both models is simply followed from consideration of solid solution parts. Let us consider pure solid solution of phase *i*. From the set of equations Eq.45 we can express factor $(1-\theta)/\theta$ as

$$\frac{1-\theta}{\theta} = \frac{1-x}{x}\mathrm{B}_2^i \exp\left(\frac{E_i^s + U_{ii}^s\theta - (E_i^b + U_{ii}^b x)}{(RT/F)}\right). \quad (56)$$

Substituting Eq.56 into Eq.46 in the case of pure phase *i* give us:

$$P_{H_2}^{eq} = RT\frac{\mathrm{B}_1^i}{\left(\mathrm{B}_2^i\right)^2}\left(\frac{x}{1-x}\right)^2 \exp\left(2\frac{E_i^b + U_{ii}^b x}{(RT/F)} - \frac{5}{2}\right) = P_i\left(\frac{x}{1-x}\right)^2 \exp\left(2\frac{E_i^b + U_{ii}^b x}{(RT/F)}\right), \qquad (57)$$

where

$$P_i = RT\frac{\mathrm{B}_1^i}{\left(\mathrm{B}_2^i\right)^2}\exp(-5/2) \qquad (58)$$

Comparing of Eq.57 with the first and third equations in the set of equations Eq.52 we can establish simple relations between parameters of LGM and Kinetic model, namely

$$U_{ii} = U_{ii}^b, \quad E_i = E_i^b \quad \text{and} \quad P_{ref} = P_i, \qquad (59)$$

First restriction is identifying one, while second and third are rather conventional normalization, since $\exp(2E_i^b/(RT/F))$ appear as multiplicative factor in front of $\mathrm{B}_1^i/\left(\mathrm{B}_2^i\right)^2$. In fact third restriction determines B_1^i given B_2^i and P_i. Thus we can conclude that Kinetic model and LGM lead to exactly the same equilibrium pressure in pure phases, while formally the kinetic model generalizes LGM in these regions.

Another interesting conclusion is followed from comparing of Eq.57 with the first and the third equations in the set of equations Eq.52. As reference pressure (P_{ref}) is temperature independent parameter, P_i also has to be temperature independent. The difference from the LGM is that in Kinetic model we expect that P_i depends on the nature of the material (Eq.59) and it also makes Kinetic model more general.

However in the phase transition region behavior of models is different. Considering set of Eqs.45(a-b) we may see, that relation $\theta = \theta(x)$ is determined by different formulas in pure phase and in two-phase coexistence region. From physical point of view, total surface coverage may not have a jump at the point of phase transition, therefore both equations in set of Eqs.45a must produce same θ at point x_α, while both Eqs.45b must produce same θ at point x_β. First condition can be written as:

$$\begin{aligned}
&\frac{\mathrm{x}_\alpha}{1-\mathrm{x}_\alpha}\quad \exp\left(\frac{E^b_\alpha + U^b_{\alpha\alpha}\mathrm{x}_\alpha}{(RT/F)}\right) = \mathrm{B}^\alpha_2 \frac{\theta(\mathrm{x}_\alpha)}{1-\theta(\mathrm{x}_\alpha)} \exp\left(\frac{E^s_\alpha + U^s_{\alpha\alpha}\theta(\mathrm{x}_\alpha)}{(RT/F)}\right), \\
&\frac{\mathrm{x}_\alpha}{1-\mathrm{x}_\alpha} \exp\left(\frac{E^s_\beta \mathrm{x}_\beta - E^s_\alpha \mathrm{x}_\alpha - U^s_{\alpha\alpha}\mathrm{x}^2_\alpha + U^s_{\alpha\beta}\mathrm{x}_\alpha\mathrm{x}_\beta/2 + L}{(RT/F)(\mathrm{x}_\beta - \mathrm{x}_\alpha)}\right) = \mathrm{B}^\alpha_2 \frac{\theta(\mathrm{x}_\alpha)}{1-\theta(\mathrm{x}_\alpha)} \exp\left(\frac{E^s_\alpha + U^s_{\alpha\alpha}\theta(\mathrm{x}_\alpha)}{(RT/F)}\right)
\end{aligned} . \qquad (60)$$

Equating left hand sides in Eq.60 we obtain continuity condition for θ at point x_α in the form:

$$(E^b_\beta \mathrm{x}_\beta - E^b_\alpha \mathrm{x}_\alpha - U^b_{\alpha\alpha}\mathrm{x}^2_\alpha + U^b_{\alpha\beta}\mathrm{x}_\alpha\mathrm{x}_\beta/2 + L)/(\mathrm{x}_\beta - \mathrm{x}_\alpha) = E^b_\alpha + U^b_{\alpha\alpha}\mathrm{x}_\alpha . \qquad (61)$$

In the similar way we obtain the second condition:

$$(E^b_\beta \mathrm{x}_\beta - E^b_\alpha \mathrm{x}_\alpha + U^b_{\beta\beta}\mathrm{x}^2_\beta - U^b_{\alpha\beta}\mathrm{x}_\alpha\mathrm{x}_\beta/2 + L)/(\mathrm{x}_\beta - \mathrm{x}_\alpha) = E^b_\beta + U^b_{\beta\beta}\mathrm{x}_\beta , \qquad (62)$$

which ensures continuity of $\theta = \theta(x)$ at point x_β. These two equations require two free variables to be solved, namely $U_{\alpha\beta}$ and L. Resolve Eqs.61,62 we obtain:

$$U^b_{\alpha\beta} = \frac{C_1 - C_2 - R_1 + R_2}{\mathrm{x}_\alpha \mathrm{x}_\beta} \quad \text{and} \quad L = \frac{C_1 + C_2 - R_1 - R_2}{2} . \qquad (63)$$

where

$$\begin{aligned}
&R_1 = E^b_\beta \mathrm{x}_\beta - E^b_\alpha \mathrm{x}_\alpha - U^b_{\alpha\alpha}\mathrm{x}^2_\alpha , \qquad && C_1 = (E^b_\alpha + U^b_{\alpha\alpha}\mathrm{x}_\alpha)(\mathrm{x}_\beta - \mathrm{x}_\alpha) , \\
&R_2 = E^b_\beta \mathrm{x}_\beta - E^b_\alpha \mathrm{x}_\alpha + U^b_{\beta\beta}\mathrm{x}^2_\beta , && C_2 = (E^b_\beta + U^b_{\beta\beta}\mathrm{x}_\beta)(\mathrm{x}_\beta - \mathrm{x}_\alpha) ,
\end{aligned} \qquad (64)$$

As we can see the set of Eqs.63,64 gives us different expressions for interaction energy between hydrogen atoms in the different phases ($U^b_{\alpha\beta}$), and the host energy (L), than we had in LGM (see Eq.34 there).

Thus, we can conclude that, generally speaking, energy parameters describing pure phases in the LGM and Kinetic Model could be the same. Moreover, the frequency factors ratios B^i_1 and B^i_2 may be chosen (normalized) in such a way that pressure relation Eq.60 in pure phases can coincide in both models.

I. Identification and estimation of surface coverage

The next very important question is estimation of the surface-hamiltonian parameters i.e. E^s_α, $U^s_{\alpha\alpha}$, E^s_β, $U^s_{\beta\beta}$. Firstly, note again, that equilibrium pressure doesn't have explicit dependence on these parameters. Secondly, E^s_α, and E^s_β enter set of Eqs.45(a-b) always in product with B^α_2 and B^β_2 and therefore cannot be identified. Thus, without loosing generality we may normalize E^s_α and E^s_β to zero and exclude them from equations. Then from Eqs.45 we obtain in two-phase region the following system of equations

$$\begin{cases} (\theta_\alpha)^2 \exp\left(\dfrac{2U^s_{\alpha\alpha}\theta^\alpha}{(RT/F)}\right) = \left(\dfrac{1-\theta_\alpha}{\mathrm{B}^\alpha_2}\right)^2 \left(\dfrac{x_\alpha}{1-x_\alpha}\right)^2 \exp\left(2H_x(x)\right) \\ (\theta_\beta)^2 \exp\left(\dfrac{2U^s_{\beta\beta}\theta^\beta}{(RT/F)}\right) = \left(\dfrac{1-\theta_\beta}{\mathrm{B}^\beta_2}\right)^2 \left(\dfrac{x_\beta}{1-x_\beta}\right)^2 \exp\left(2H_x(x)\right) \end{cases}, \tag{65}$$

where

$$H_x(x) = F(E^b_\beta \mathrm{x}_\beta - E^b_\alpha \mathrm{x}_\alpha - U^b_{\alpha\alpha}\mathrm{x}^2_\alpha \mathrm{v}_\alpha + U^b_{\beta\beta}\mathrm{x}^2_\beta \mathrm{v}_\beta + U^b_{\alpha\beta}\mathrm{x}_\alpha \mathrm{x}_\beta(\mathrm{v}_\alpha - \mathrm{v}_\beta)/2 + L)/RT/(\mathrm{x}_\beta - \mathrm{x}_\alpha).$$

Substituting Eqs.65 into second equation of Eq.46 we obtain

$$P^{eq}_{H_2} = \frac{Z_\alpha(1-\theta_\alpha)^2 \mathrm{v}_\alpha + Z_\beta(1-\theta_\beta)^2 \mathrm{v}_\beta}{(1-\theta_\alpha)^2 \mathrm{v}_\alpha + (1-\theta_\beta)^2 \mathrm{v}_\beta} \exp\left(2H_x(x)\right), \tag{66}$$

where $Z_i = P_i \left(\dfrac{x_i}{1-x_i}\right)^2$. We can see that equilibrium pressure in the two-phase transition region indeed depends on $U^s_{\alpha\alpha}$, $U^s_{\beta\beta}$, B^α_2 and B^β_2 (indirectly via θ-s). Therefore these four parameters can be estimated via the data, and then used to find the surface coverage.

Let us observe now, that "pseudo-pressures" P_i in Eq.57 and Eq.66 are still not identified separately, since multiplication of both parameter by the same number may be exactly compensated by (same) additive term in E^b_α and E^b_β. To avoid identification problem and stress relation with LGM we set $P_\alpha = P_{ref}$ in estimations.

J. Case of immediate phase transition

As we have seen in previous section parameters related to surface Hamiltonian and adsorption/absorption rate constants are estimated only by plateau data. It is of interest to check what happens if the plateau is absent. First, note, that in absence of phase transition we can estimate neither surface coverage nor parameters of surface Hamiltonian. Indeed, suppose that only α-phase is present. Then Eq.57 directly give us dependence of pressure on state of charge, and these relations do not involve θ, U_{ii}^{s}. When we estimate parameters of Eqs.57 we may use equation Eq.56 to determine θ. That, however, require knowledge of U_{ii}^{s}. For any values of these parameters we obtain certain value of θ. But since U_{ii}^{s} is not estimable (and therefore not known), the θ also not known.

In the case of instantaneous phase transition we have one single phase transition point x_t. Below that value in the bulk only α-phase is present, above there is only β-phase. Then, according to Eq.57 we obtain:

$$P_{H_2}^{eq} = \begin{cases} P_\alpha \left(\frac{x}{1-x}\right)^2 \exp\left(2\frac{E_\alpha^b + U_{\alpha\alpha}^b x}{(RT/F)}\right), & x < \mathrm{x}_t, \\ P_\beta \left(\frac{x}{1-x}\right)^2 \exp\left(2\frac{E_\beta^b + U_{\beta\beta}^b x}{(RT/F)}\right), & x > \mathrm{x}_t. \end{cases} \tag{67}$$

We must impose restriction on parameters of the model, ensuring continuity of pressure at point x_t. Make equal both branches of Eq.67 at x_t resolving it with respect to E_β^b we obtain:

$$E_\beta^b = E_\alpha^b - (U_{\beta\beta}^b - U_{\alpha\alpha}^b)\mathrm{x}_t + \frac{RT}{F}\log\left(\frac{P_\alpha}{P_\beta}\right). \tag{68}$$

Substitution of restriction Eq.68 to Eq.67 gives us:

$$P_{H_2}^{eq} = P_\alpha \left(\frac{x}{1-x}\right)^2 \exp\left(\frac{2E_\alpha^b}{(RT/F)}\right) \begin{cases} \exp\left(\frac{2U_{\alpha\alpha}^b x}{(RT/F)}\right), & x < \mathrm{x}_t, \\ \exp\left(\frac{2U_{\alpha\alpha}^b x_t}{(RT/F)}\right)\exp\left(2\frac{U_{\beta\beta}^b (x - x_t)}{(RT/F)}\right), & x > \mathrm{x}_t. \end{cases} \tag{69}$$

Now consider continuity condition for surface coverage. Equating both branches of Eq.66 in phase transition point x_t we can express

$$(U^s_{\beta\beta} - U^s_{\alpha\alpha})\theta(x_t) = \frac{RT}{F}\log(\frac{B^{\alpha}_2}{B^{\beta}_2}).$$

Then, using restriction condition Eq.68 and definition Eq.58 we obtain:

$$(U^s_{\beta\beta} - U^s_{\alpha\alpha})\theta(x_t) = -\frac{RT}{2F}\log(\frac{B^{\alpha}_1}{B^{\beta}_1}) + \frac{1}{2}(E^b_{\beta} - E^b_{\alpha} + (U^b_{\beta\beta} - U^b_{\alpha\alpha})x_t), \qquad (70)$$

that defines value of the surface coverage at point x_t, i.e. $\theta(x_t)$, providing $U^s_{\beta\beta} - U^s_{\alpha\alpha} \neq 0$. Substituting $\theta(x_t)$ into each branch of Eq.56 we obtain equation for U^s_{ii}. Thus, all necessary parameters are identified in that case. However if $U^s_{\beta\beta} = U^s_{\alpha\alpha}$ then any value of $\theta(x_t)$ is a solution of Eq. 70, thus θ is not identifiable.

3. RESULTS AND DISCUSSION

The presented equilibrium kinetic model has been tested, using the experimental data reported for various AB_5-type hydrogen storage materials. These materials have been thoroughly characterized with respect to their physical and electrochemical performance. The isotherms for both model-type materials and commercial, MischMetal-based, hydride-forming materials have been simulated as a function of composition and temperature, respectively. Since all considered materials have the same, hexagonal, crystallographic structure for both the α- and β phase it is evident that the number of host sites per unit cell remains constant, *i.e.* parameters d^b (and d^s) is considered unity in the present simulations.

The experimental absorption isotherms have been measured with a conventional "Sieverts-type" apparatus by expanding a known amount of gas or vacuum into an *in situ* XRD cell and allowing the system to come to equilibrium after each pressure change[19]. The *in situ* XRD measurements allowed obtaining crystallographic information of the system as a function of the hydrogen content.

It is well known that (non-)stoichiometric hydride-forming materials are stable with respect to hydrogen storage[18,19]. The crystallographic structure of these materials has been illustrated in Fig.3. These materials have a rather simple composition and can therefore be considered as model systems for which the phase transitions can be well controlled by the stoichiometric composition.

Fig.8 shows the agreement between the experimentally measured (symbols) and simulated (line) pressure-composition isotherm (left-hand axis) and the corresponding equilibrium potential curve (right-hand axis) for the stoichiometric $LaNi_{4.0}Cu_{1.0}$. In this specific stoichiometric case no dumbbell pairs have been introduced in the host crystal lattice (see Fig.3). The solid line represents the simulation according to the Eq.45,46. The numerical values of the parameters of the model were obtained by nonlinear least-squares method and are listed in Table I. Some explanation concerning the estimation scheme is as following. In the course of estimation we tried to force connection with the LGM[13]. By that reason some of the parameters, namely x_α, x_β, E^b_α, $U^b_{\alpha\alpha}$ and $U^b_{\beta\beta}$ had been directly taken from LGM estimation (appropriate parameters of the LGM are shown in the Table II). Surface energy parameters, namely E^s_α, E^s_β, $U^s_{\alpha\alpha}$ and $U^s_{\beta\beta}$ were set to zero since they are not identifiable. By the same reason B^β_2 was set to one. Value P_α was set to normal atmospheric pressure (10^5 Pa). As parameters Π^i_{jk} are relative and unidentifiable in our system they have been set by zero. Three remaining parameters B^α_2, E^b_β and P_β were estimated by nonlinear least-squares. In fact we have described whole pressure composition isotherm by just three adjustable parameters. As Fig. 6 reveals, the kinetic model describes the isotherm quite well for the stoichiometric $LaNi_{4.0}Cu_{1.0}$ material. Three regions can be clearly distinguished: Nernst-type solid solution region for low hydrogen concentration ($x < 0.196$), a long, almost flat, two-phase coexistence plateau region ($0.196 \le x \le 0.794$), and Nernst-type solid solution region for high hydrogen concentration ($x > 0.794$). However the LGM is also capable to describe the pressure-composition isotherm quite well. What can kinetic model add to this description?

The distinctive feature of the model is its ability to reveal information about chemical kinetics of the processes. At Fig.9 and 10 we can see equilibrium rates for two basic reactions considered in the paper. Fig.9 shows dissociation and recombination rates i.e. rates corresponding to the Eq.2. Note that positive sign of the direct reaction rate corresponds to the flux from the gas phase into the alloy. We can see that dissociation and recombination rates are the same in absolute values but have opposite signs as it must be in equilibrium. The equality of direct and reverse reaction rates in Eq.2 (direct and reverse rate balance Eq.17) gives us condition determining the equilibrium pressure in Eq.18. We may observe that reaction rate is small in the very initial part of the α phase solid solution region. When hydrogen concentration inside the alloy (and outside it as well) grows, the

dissociation rate also grows and reach it's maximum near the first phase transition point x_α. In the two-phase coexistence region this rate goes down significantly until reach it's minimum in x_β. In the β-solid solution region it remains practically constant and concentration independent. We may conclude, that *gas-surface* kinetics in the α-phase is, in general, faster than in the β-phase.

This conclusion holds also for absorption-desorption reaction. Indeed, from Fig.10 we can see, that shape of the equilibrium absorption and desorption rates is similar to those at Fig.9. That implies fast bulk kinetics in the α-phase and slow kinetics in the β-phase. Also, due to strong influence of phase separation in the bulk and surface of the hydride-forming material the shape of the absorption and desorption reaction rates is more complicated that those of the dissociation-recombination reaction (see Fig.9). Absorption rate depicted in Fig.10 has two maxima in the phase transition points and minimum in the two phase coexistence region.

Let us analyze equilibrium reaction rates in more details. Fig.11 presents detailed composition of the total dissociation rate into rates via surfaces of α- and β-phase. Naturally, in pure α-phase whole rate (red line) coincides with the α-rate (green line). As soon as phase transition occurs, surface of the α-phase gradually diminishes in favor of the β-phase. Consequently, the share of α-phase in total flux reduces (green lines goes down fast). At the end of the two-phase coexistence region the total flux is composed of the flux via surface of β-phase only. At the Fig.12 we may observe normalized (per unit of squared surface of particular phase) dissociation rates in both phases. Again we can see, that rate of hydrogen dissociation in α-phase is negligible when hydrogen concentration is small, then it increases and reaches maximum near the point of phase transition. In the two-phase area it is constant and larger than rate of β-phase. The hydrogen dissociation rate of the β-phase is practically constant both in the two-phase coexistence region and in the β solid solution region.

Similar to the dissociation-recombination reaction the adsorption rate in α-phase (see Fig.13) increases with hydrogen concentration and reaches maximum near the left phase transition point x_α. In two phase coexistence region due to the competition of reaction rates in α (green line) and β (blue line) phase, the minimum in the total reaction rate (red line) is observed. Adsorption rate in β-phase is smaller than in α-phase. However in the β-phase behavior of the absorption rate is different from the dissociation

rate of the dissociation-recombination reaction: it gradually decreases toward zero, while dissociation rate keeps its level. The same behavior was observed for desorption rate.

Fig.14, where we have plotted normalized adsorption rates completes the analysis. We may see that both α and β normalized rates are constant in the two-phase region and former is smaller than later. Normalized β rate declines quickly as hydrogen concentration approach maximum. Physical sense behind that behavior is simple. Both very large and very small hydrogen concentrations hinder absorption kinetic. Apparently it is difficult to absorb hydrogen into the bulk if there is no place there. Similarly it is difficult to desorp hydrogen from the bulk if there is almost no hydrogen there. Note that absorption and desorption rates are equal in equilibrium. So the subsurface kinetic is sensitive to extreme concentrations of hydrogen. In case of dissociation-recombination situation is different. The redundancy of the hydrogen in the bulk does not influence rates of the reactions with the surface layer, at least if the surface coverage is not one. But these rates decrease if normalized hydrogen concentration goes to zero.

One of the contributions of the paper is the new approach of the rate constant description. The classical Langmuir approach treats the rate constants as constants. We may see that in our system for moderate hydrogen concentrations in the surface of the hydride-forming material this is correct (we set surface energy parameters E_{α}^{s}, E_{β}^{s}, $U_{\alpha\alpha}^{s}$ and $U_{\beta\beta}^{s}$ to zero since they are not identifiable). However, for the bulk rate constants (desorption rate constants), namely k_{-2}^{α}, k_{-2}^{β} there are some substantial deviations in the behavior for extreme hydrogen concentrations. Dependence of these constants on the hydrogen concentration is shown in Fig.15. Very small and very large hydrogen concentrations significantly change desorption rate constants, while in the two phase coexistence plateau region they are equal and almost not sensitive to the hydrogen concentrations. We may say that our rate constant approach generalizes nicely classical approach, and at the same time confirms that classical approach is also valid to moderate hydrogen concentrations in some areas of our system.

Since kinetics in the β-phase is slow, we expect the larger percentage of the surface to be covered there. Fig.16 illustrates dependence of surface coverage on state of charge. We may see that, in general, surface coverage increases with the state of charge, while somewhat differently in three regions. It is interesting to point out that in considering system the surface coverage demonstrates the similar behavior as the pressure composition isotherm. In two solid solution region it has non-linear (logarithmic) shape

while in the two phase coexistence region it shows linear behavior, but in contrary with isotherms the slope of the surface coverage in the two phase region much more bigger.

The next plot, Fig.17, shows the pressure composition isotherms for all four materials under consideration. We can see that model perfectly adapts to the variety of the shapes caused by different material compositions. The dotted line in the Fig.17 corresponds to $LaNi_{5.0}Cu_{1.0}$, where we observe instantaneous phase transition.

At Fig.18 we may observe, how the surface coverages change with the increase of the degree of non-stochiometry (parameter *y* in formula $LaNi_yCu_{1.0}$). In particular we can see that surface coverage at the plateau is higher for materials with higher plateau pressure that corresponds to the common physical sense. For large hydrogen concentrations, at the end of β solid solution region, the surface coverage behaves in opposite way, i.e. it is decreasing with the increase of the degree of non-stochiometry. This suggests faster β-phase kinetics for these materials. Note that $LaNi_{5.0}Cu_{1.0}$ is not presented at the figure, since surface coverage can not be estimated for this case. These preliminary conclusions are confirmed by detailed analysis of normalized recombination rates for three model material i.e. Fig.19. There we can see that kinetics in α-phase declines when y grows, while in β-phase situation is reverse. For $LaNi_{4.0}Cu_{1.0}$ the difference between the rates of α- and β- phases is maximal. When *y* grows this gap gradually reduces and became negligible for $LaNi_{4.4}Cu_{1.0}$. The same pattern is revealed for adsorption rate in Fig.20. The only substantial difference is that normalized absorption rates go down for large hydrogen concentrations. Also kinetics in β phase becomes faster than that in α phase in two phase coexistence region for $LaNi_{4.4}Cu_{1.0}$ stoicheometric alloy. We did not show the phase diagram for estimated parameter values, since it is exactly coincides with one reported in the LGM paper[13].

Some analysis of parameter estimates is the following. Estimated values of E_x^β are somewhat higher than their counterparts from LGM, but are in reasonable physical range. We may also observe that frequency related parameter B_2^α declines with the degree of non-stochiometry. Since $B_2^\alpha = B_2^\alpha / B_{-2}^\alpha$, we may say that frequency factor for desorption reaction became larger than for absorption one. We did not reported estimated parameter values for $LaNi_{5.0}Cu_{1.0}$ material, since those are exactly equals to their counterparts in the LGM. Also it is very interesting to point out that reference pressure parameter $P^{(\beta)}$ which in the LGM is equal that in the α phase and set to the normal atmospheric pressure (10^5

Pa) in our kinetic model growth with increasing of non-stoicheometry. That makes the kinetic model more general, flexible and close to reality.

Good performance of the model does not restricted by the model materials. Simulation of the MischMetal-based commercial materials[29,30] produced by Matsushita Corp for various temperatures (0, 24, 45, 60 and 70°C) is shown in Fig.21. Again, model adapts well to the range of experimental curves. As expected, the plateau pressure increases with increasing temperatures. Fig.22 illustrates surface coverages for the range of available temperatures. We can clearly observe that surface coverage becomes larger for higher temperature that is in line with generally accepted Langmuir consideration. As we expected surface kinetics of the alloy accelerates with temperature as shown in Fig.23. The similar behavior can be seen in Fig.24 where equilibrium absorption-desorption rates are plotted. We may observe that influence of the temperature is maximal in α-phase, but declines in β-phase. This observation is confirmed by analysis of the normalized concentrations for two basic reactions given in Fig.25 and 26. The acceleration effect is more visible in the surface reaction in the α-phase. We may also point out that normalized absorption rates in α and β - phases became equal approximately at 60°C.

We should note that estimation scheme for the MischMetal-based commercial materials was somewhat different from one employed for LaNi-based stoicheometric materials. The sample measured at 24°C was estimated in the same way as all LaNi alloys. In particular, parameter P_α was set to normal atmospheric pressure (10^5 Pa). For other temperatures this parameter had been estimated, otherwise fit was poor. All obtained model parameter values are given in the Table.III. Behavior of the estimated P_α and P_β as functions of temperature is shown in Fig.27: almost linear dependence (in a log-scale) is observed. Estimated energies are all in physically meaningful range and mostly keep the same behavior as in the LGM (absolute values increases with temperature). The difference in estimated values between LGM and kinetic model is minor with one exception: estimates for parameter L are of the opposite signs estimation (appropriate parameters of the LGM are shown in the Table IV). This, however, is of marginal concern since absolute values of L are one-two orders of magnitude smaller than other energy related parameters.

4. CONCLUSIONS

In the present paper the new equilibrium kinetic model describing hydrogen storage in the hydride forming materials has been proposed. The model is based on the first principles of chemical kinetics, statistical mechanics and reasonable structural assumptions.

A complete set of equations, describing pressure-composition isotherms including phase transformation has been obtained. The model defines the equilibrium pressure as a function of the normalized surface coverage θ and normalized hydrogen concentration x, with parameters, namely the phase-transition points, interaction energies between atoms, the host energy, ect. The final set of equations consists of three parts; the first ($x < x_{\alpha}$) and last ($x > x_{\beta}$) parts characterize the solid solution regions of the pure α and β phases, respectively, and have the Nernst-type logarithmic form the second equation is responsible for two phase coexistence region.

The new approach of description of the chemical rate constants has been given. Approach generalizes classical Langmiur and Temkin approaches and based on clear energy description of the system ("rectangle rule"). The strong general energy description of each area of the system including surface and gas phase has been given. Estimation results show that the rate constants are indeed deviates from constant for extreme values of concentrations. Proposed approach can be applied not only in hydrogen storage system but to any considered reacting system. Case of immediate phase transition also has been described.

Paper contains explicit comparison between earlier published Lattice Gas Model and nicely completes thermodynamic description presented there by accessing various aspect of the hydrogen storage equilibrium kinetics.

Simulations of experimental absorption isotherms have been presented for both model hydride-forming $LaNi_yCu_{1.0}$-type materials and commercial MischMetal-based hydrogen storage electrode materials. The experimental and theoretical results of the equilibrium hydrogen pressure show good agreement. The calculated pressure-composition isotherms at various temperatures also show a good agreement with the experiments.

The simulation results shows that during hydrogen storage process three regions can be clearly distinguished: Nernst-type solid solution region for low hydrogen concentration, two-phase coexistence plateau region, and Nernst-type solid solution region for high hydrogen concentration.

After deep consideration chemical kinetics of all areas in our reacting system, we may conclude, that gas-surface kinetics in the α-phase, in general, is faster than that of in the β-phase. This conclusion holds also for absorption-desorption (surface-bulk) reaction. Absorption-desorption rate has two maxima in the phase transition points and minimum in the two phase coexistence region. Also it was shown that hydrogen storage kinetics is sensitive to extreme concentrations of hydrogen.

Surface coverage increases with the state of charge, while somewhat differently in three regions, and demonstrates the similar behavior as the pressure composition isotherm. It was shown that surface coverage at the plateau region is higher for materials with higher plateau pressure and higher order of non-stoicheometry.

As expected, the plateau pressure increases with increasing temperatures and surface coverage becomes larger for higher temperature that is in line with generally accepted Langmuir consideration. Also surface and bulk kinetics of the hydride-forming material accelerates with temperature.

We may say that our approach to describe kinetics of hydrogen storage in hydride-forming materials nicely generalizes classical approach, and makes the kinetic model more general, flexible and close to reality.

ACKNOWLEDGEMENTS

The authors would like to thank Prof. dr. T.B. Flanagan (University of Vermont, USA) for stimulating and helpful discussions.

REFERENCES

[1] Y. Fukai, *The Metal-Hydrogen System* (Springer-Verlag, Berlin Heidelberg, 1993).
[2] T.B. Flanagan, *Thermodynamics of metal-gas reactions* (Interstitial Intermetallic Alloys, Kluwer Acad. Publish., 1995), p.43.
[3] P.H.L. Notten, *Interstitial intermetallic alloys*, Chapter 7 NATO (1995), edited by F. Grandjean, G.J. Long and K.H.J. Buschow, ASI Series Vol. E281 (NATO, 1995), Chap.7.
[4] P.H.L. Notten and M. Latroche, *Nickel-MetalHydride batteries: a successful application of hydrogen storage materials* (Encyclopedia of Electrochemical Power Sources, in press 2007).
[5] L. Schlapbach and A. Zuttel, Nature **414,** 353 (2002).
[6] K.H.J. Buschov, P.C.P. Bouten and A.R. Miedema, Rep. Prog. Phys. **45,** 937 (1982).
[7] R. Griessen, T. Riesterer, *Heat formation models*, edited by L. Schlapbach, Topics in Applied Physics (Springer-Verlag, Berlin, 1988) p. 219.
[8] L. Schlapbach, *Surface properties and activation*, edited by L. Schlapbach, Topics in Applied Physics (Springer-Verlag, Berlin, 1992) p. 15.

[9] H. Frieske and E. Wicke, Ber. Bunsenges. Phys. Chem., **77,** 48 (1973).
[10] Y. Sakamoto, E.Kakihisa, and Y.Kinari, Zeitschrift fur Phys. Chem., Bd., **179,** 69 (1993).
[11] A. Ledovskikh, E. Verbitskiy, A. Ayeb, and P.H.L. Notten, J. Alloys Comp., **356-357**, 742 (2003).
[12] T.B. Flanagan, W.A. Oates, Top. Appl. Phys., **63,** 49 (1988).
[13] A. Ledovskikh, D. Danilov, W.J.J. Rey and P.H.L. Notten, Phys. Rev. B, **73,** 014106, 1, (2006).
[14] J.R. Lacher, Proc. Cambr. Phil. Soc., 33, 518 (1937).
[15] M. V. Lototsky, V. A. Yartys, V. S. Marinin and N. M. Lototsky, J. Alloys Comp., 356-357, 27 (2003).
[16] S. Naito, M.Yamamoto, M.Doi and M.Kimura, J. Chem. Soc., Far. Trans., 22, 4143 (1995).
[17] E. Gileadi, B.E. Conway, *"The behaviour of intermediates in electrochemical catalysys, in "Modern aspects of electrochemistry"*, ed. J,O'M. Bockris, B.E. Conway, **N3** (1964), London, Butterworth.
[18] E. Gileadi, *"Adsorption in Electrochemistry"*, Chapt. 1, in *"Electrosorption"*, ed. E. Gileadi, Plenum Press, NY (1967).
[19] F. Feng, M. Geng, D.O.Northwood, Comp. Mat. Sc., **23**, 291 (2002).
[20] W. Coene, P.H.L. Notten, F. Hakkens, R.E.F. Einerhand and J.L.C. Daams, Phil. Mag. A, 65, 1485 (1992).
[21] M. Latroche, J.M. Joubert, P.H.L. Notten and A. Percheron-Guegan, J. Sol. State Chem., 146, 313 (1999).
[22] A.J. Bard and L.R. Faulkner, Electrochemical Methods, Fundamentals and Applications, Wiley, N.Y. (1980).
[23] M.I Temkin and V. Pyzhev, Acta Physicochimica USSR, XII, 3, 327 (1940).
[24] Frumkin, Z. Physic. Chem., 116, 466 (1925).
[25] P.H.L. Notten, R.E.F. Einerhand and J.L.C. Daams, J. Alloys Comp., 210, 221 (1994).
[26] P.H.L. Notten, J.L.C. Daams and R.E.F. Einerhand, J. Alloys Comp., **210,** 233 (1994).
[27] T.L. Hill, *An introduction to statistical thermodynamics* (Addison-Wesley, 1960).
[28] R. Kubo, *Thermodynamics: an advanced course with problems and solutions*, Amsterdam North Holland (1968
[29] H. Senoh, K. Morimoto, H. Inoue. C. Iwakura and P.H.L. Notten, J. Electrochem. Soc., **147,** 2451 (2000).
[30] Y. Dansui and P.H.L. Notten, private communications.

Table 1. Simulation results for the equilibrium kinetic model
(stoichiometric and non-stoichiometric materials).

N	Par	Dim	$LaNi_{4.0}Cu_{1.0}$	$LaNi_{4.2}Cu_{1.0}$	$LaNi_{4.4}Cu_{1.0}$
1	x_α	$[1]^*$	0.196	0.231	0.276
2	x_β	$[1]^*$	0.794	0.711	0.448
3	E_α^b	$[10^{-2}\,\mathrm{eV}]^*$	6.900	7.000	7.200
4	E_β^b	$[10^{-2}\,\mathrm{eV}]$	**7.912**	**6.709**	**7.417**
5	$U_{\alpha\alpha}^b$	$[10^{-1}\,\mathrm{eV}]^*$	-1.580	-1.390	-1.220
6	$U_{\beta\beta}^b$	$[10^{-2}\,\mathrm{eV}]^*$	-5.300	-4.200	-8.000
7	$U_{\alpha\beta}^b$	$[10^{-1}\,\mathrm{eV}]^\#$	-2.499	-1.725	-2.050
8	L	$[10^{-2}\,\mathrm{eV}]$	-1.318	-0.659	-0.338
9	B_1^α	$[10^4]^\#$	1.017	0.131	0.017
10	B_1^β	$[10^2]^\#$	0.024	0.090	1.163
11	B_2^α	**[1]**	**4.509**	**1.615**	**0.580**
12	B_2^β	$[1]^+$	1.000	1.000	1.000
13	P_α	$[10^5\,\mathrm{Pa}]^+$	1.000	1.000	1.000
14	P_β	$[10^4\,\mathrm{Pa}]$	**0.047**	**0.181**	**2.325**
15	E_α^s	$[\mathrm{eV}]^+$	0.000	0.000	0.000
16	E_β^s	$[\mathrm{eV}]^+$	0.000	0.000	0.000
17	$U_{\alpha\alpha}^s$	$[\mathrm{eV}]^+$	0.000	0.000	0.000
18	$U_{\beta\beta}^s$	$[\mathrm{eV}]^+$	0.000	0.000	0.000

parameters in **bold** are obtained by optimization
*parameter values are taken from the Lattice Gas Model
#parameters are calculated from the continuity conditions.
+parameters are set to constant by normalisation

Table 2. Lattice Gas Model. Simulation results for stoichiometric and non-stoichiometric materials

Composition	*Experimental*		*Simulation*							
	x_α	x_β	x_α	x_β	E_α [eV]	E_β [eV]	$U_{\alpha\alpha}$ [eV]	$U_{\beta\beta}$ [eV]	$U_{\alpha\beta}$ [eV]	L [eV]
$LaNi_{4.0}Cu_{1.0}$	0.11	0.76	0.196	0.794	0.069	0.011	-0.158	-0.053	-0.257	0.020
$LaNi_{4.2}Cu_{1.0}$	0.19	0.67	0.231	0.711	0.070	0.017	-0.139	-0.042	-0.181	0.017
$LaNi_{4.4}Cu_{1.0}$	0.33	0.41	0.276	0.448	0.072	0.056	-0.122	-0.080	-0.206	0.003
$LaNi_{5.0}Cu_{1.0}$	0.36	0.36	0.346	0.346	0.046	0.069	-0.026	-0.092	-	-0.003

Table 3. Simulation results for Matsushita commercial materials.

N	Par	0°C	24°C	45°C	60°C	70°C
1	x_α *	0.184	0.211	0.208	0.235	0.229
2	x_β *	0.581	0.556	0.596	0.603	0.603
3	$E_\alpha^b\,[10^{-2}\,\mathrm{eV}]$	**0.846**	3.700*	**4.538**	**5.183**	**5.635**
4	$E_\beta^b\,[10^{-2}\,\mathrm{eV}]$	**0.383**	**2.651**	**4.606**	**5.282**	**6.526**
5	$U_{\alpha\alpha}^b\,[10^{-1}\,\mathrm{eV}]$ *	-0.460	-1.150	-1.230	-1.250	-1.280
6	$U_{\beta\beta}^b\,[10^{-2}\,\mathrm{eV}]$ *	-0.700	-2.500	-4.500	-5.100	-6.400
7	$U_{\alpha\beta}^b\,[10^{-1}\,\mathrm{eV}]$ #	-0.358	-1.092	-1.701	-1.786	-2.161
8	$L\,[10^{-3}\,\mathrm{eV}]$ #	-0.312	-1.257	-5.110	-5.659	-8.128
9	$B_1^\alpha\ [10^3]$ #	0.442	0.508	0.644	0.853	1.013
10	$B_1^\beta\ [10^1]$ #	2.444	3.222	3.347	5.171	5.534
11	B_2^α +	1.000	1.000	1.000	1.000	1.000
12	B_2^β +	1.000	1.000	1.000	1.000	1.000
13	$P_\alpha\ [10^5\,\mathrm{Pa}]$	**0.824**	1.000+	**1.397**	**1.918**	**2.371**
14	$P_\beta\ [10^4\,\mathrm{Pa}]$	**0.455**	**0.653**	**0.747**	**1.196**	**1.332**
15	$E_\alpha^s\,[\mathrm{eV}]$ +	0.000	0.000	0.000	0.000	0.000
16	$E_\beta^s\,[\mathrm{eV}]$ +	0.000	0.000	0.000	0.000	0.000
17	$U_{\alpha\alpha}^s\,[\mathrm{eV}]$ +	0.000	0.000	0.000	0.000	0.000
18	$U_{\beta\beta}^s\,[\mathrm{eV}]$ +	0.000	0.000	0.000	0.000	0.000

parameters in **bold** are obtained by optimization
*parameter values are taken from the Lattice Gas Model
#parameters are calculated from the continuity conditions.
+parameters are set to constant by normalization

Table 4. Lattice Gas Model. Simulation results for Matsushita materials

Temperature [°C]	x_α	x_β	E_α [eV]	E_β [eV]	$U_{\alpha\alpha}$ [eV]	$U_{\beta\beta}$ [eV]	$U_{\alpha\beta}$ [eV]	L [eV]
0	0.184	0.581	0.005	-0.033	-0.046	-0.007	-0.071	0.011
24	0.211	0.556	0.037	-0.009	-0.115	-0.025	-0.123	0.012
45	0.208	0.596	0.049	0.010	-0.123	-0.045	-0.194	0.010
60	0.235	0.603	0.060	0.022	-0.125	-0.051	-0.196	0.010
70	0.229	0.603	0.068	0.036	-0.128	-0.064	-0.235	0.009

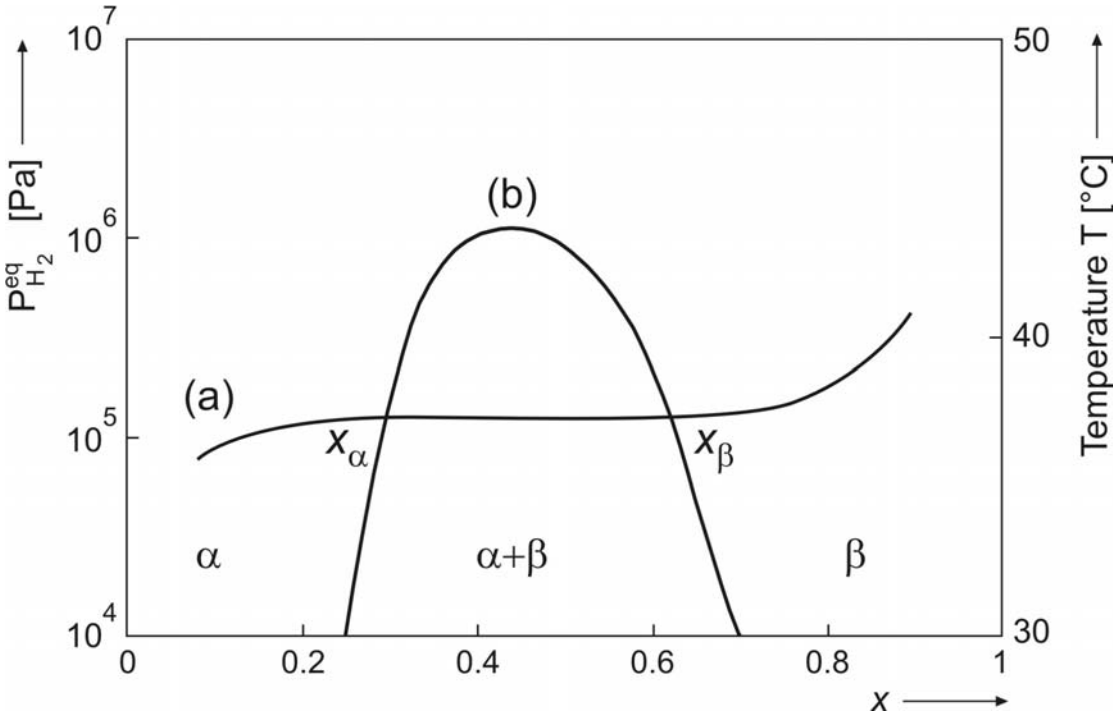

FIG. 1. Schematic representation of a pressure-composition isotherm (a) and phase-diagram (b) for a typical hydrogen storage material. The α and β solid-solution regions are indicated together with the temperature-dependent two-phase (α+β) miscibility gap.

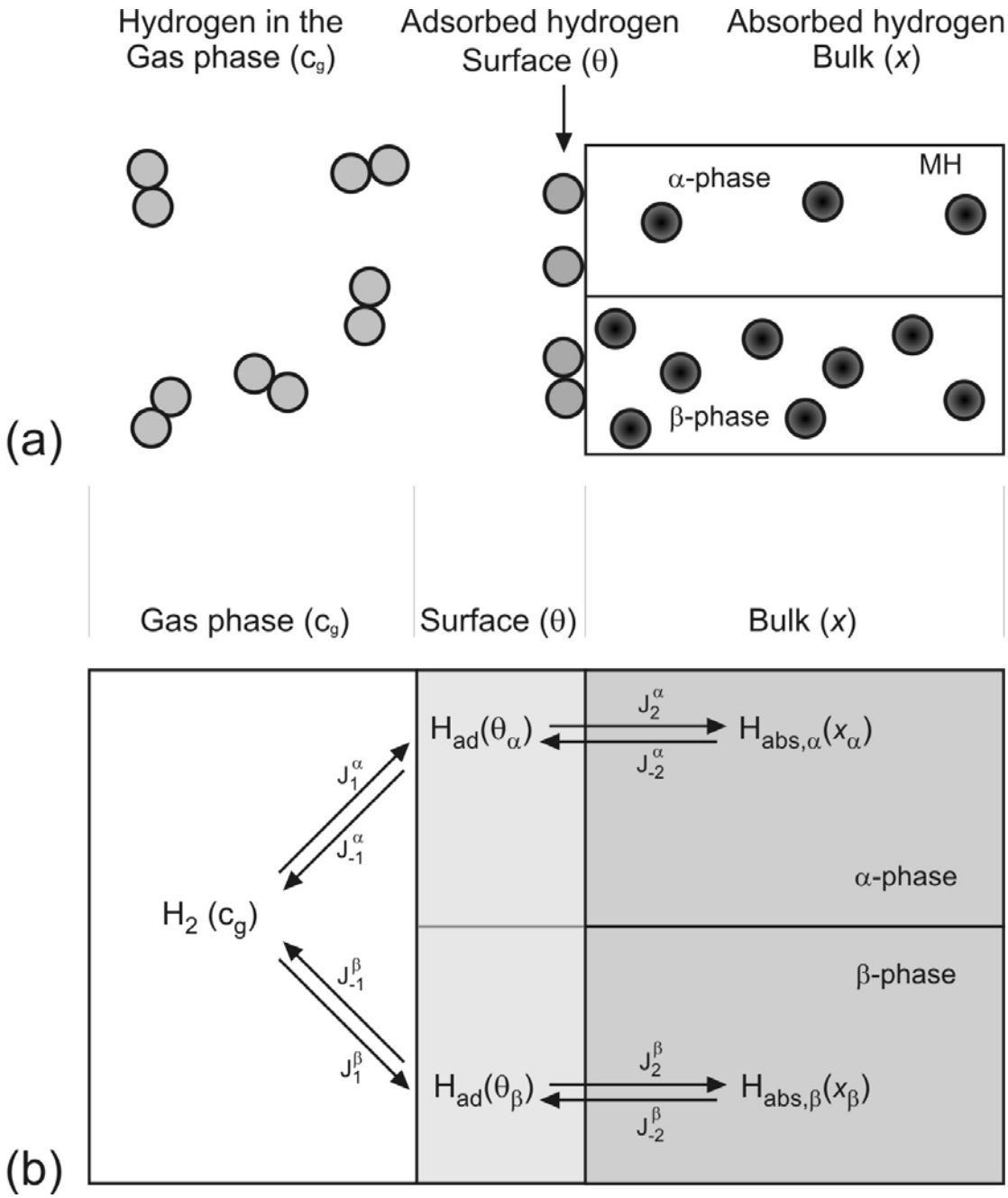

FIG. 2a. Schematic representation of the hydrogen storage process. **b.** General (de)hydrogenation reaction scheme, including the dissociation and recombination reaction at the surface and the hydrogen absorption and desorption in the bulk of the hydride-forming material.

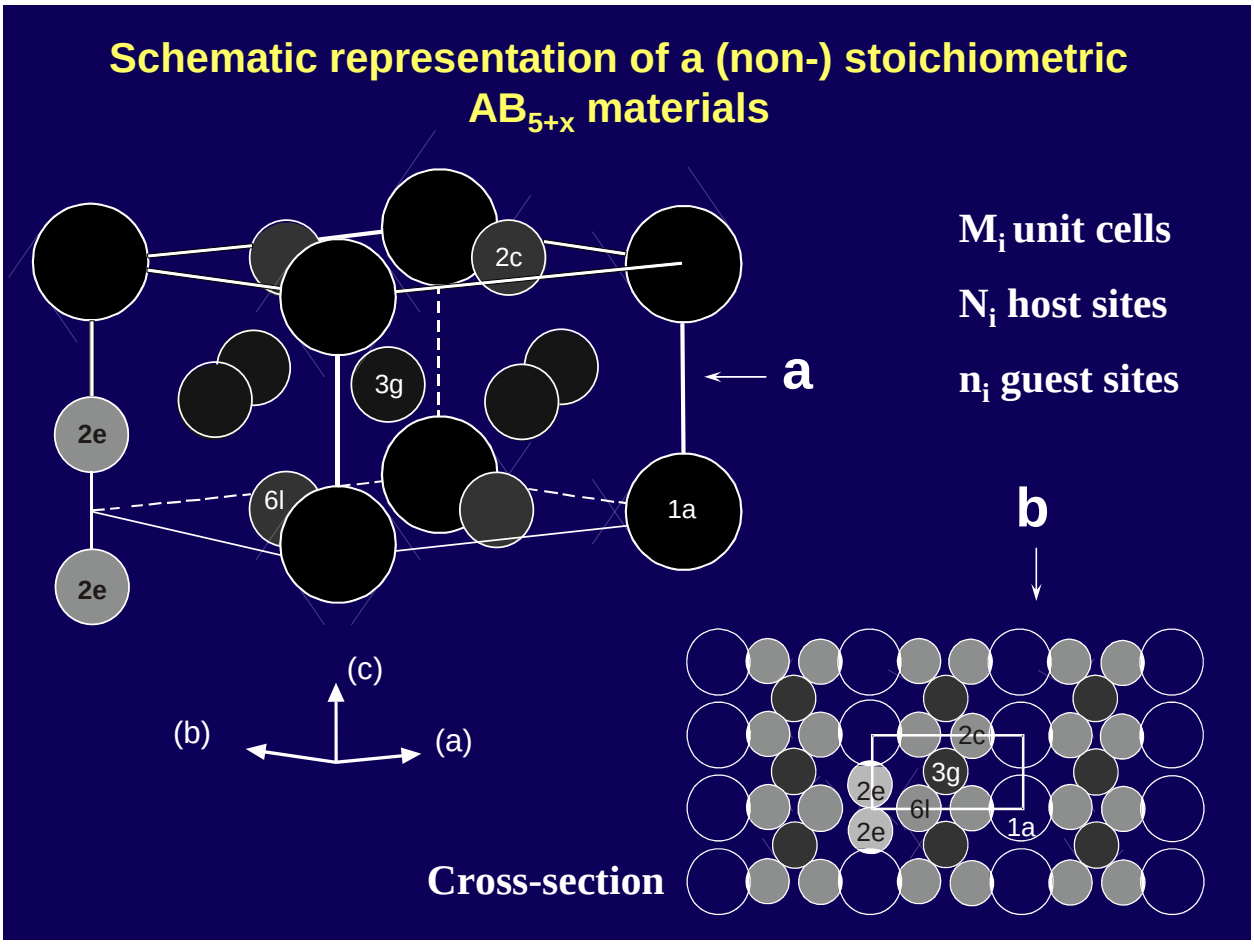

FIG.3. Schematic representation of a non-stoichiometric AB_{5+x} unit cell (a) and corresponding cross-sectional view (b). The large and small atoms represent the A- and B-type atoms, respectively[4].

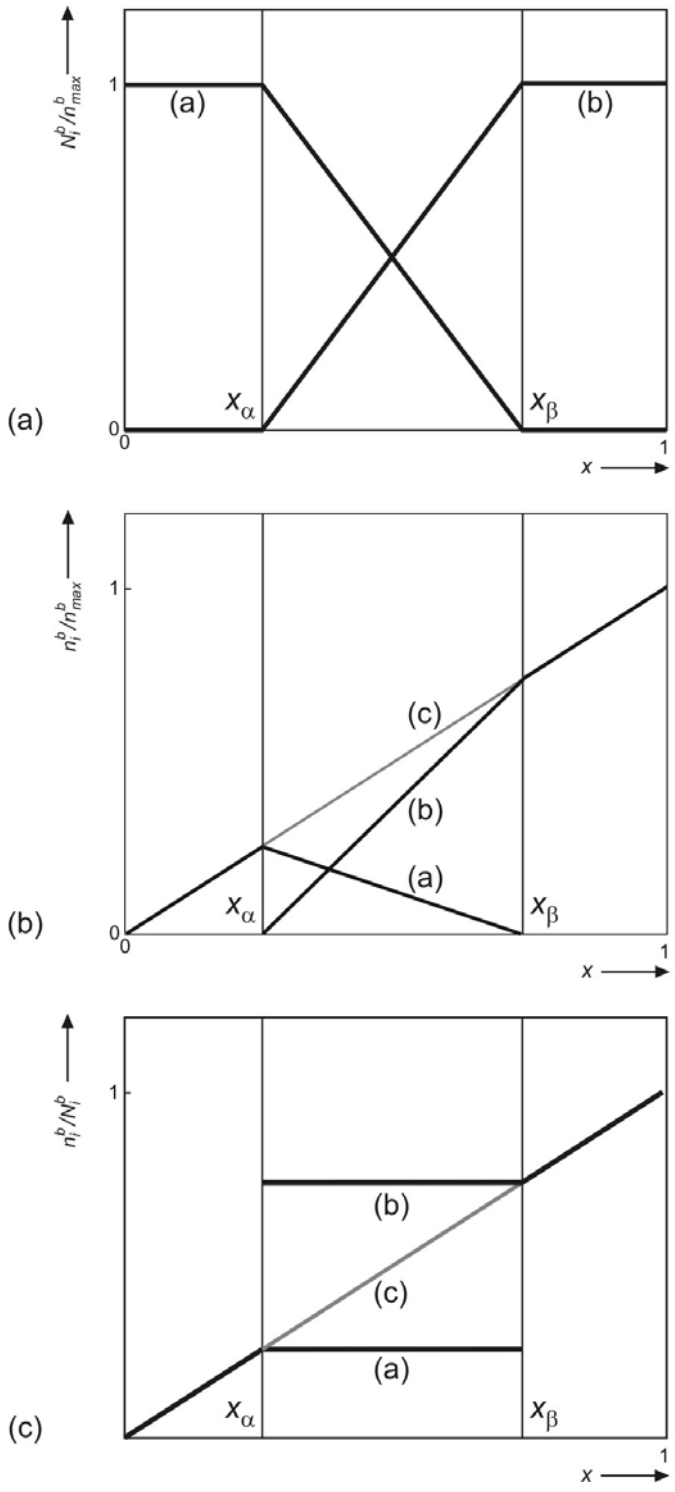

FIG. 3a. Normalized number of host sites (N_i^b / n_{max}^b) as a function of normalized hydrogen concentration (x) in the α- (curve (a)) and β-phase (curve (b)). **b.** Partial hydrogen concentrations ($x^i = n_i^b / n_{\max}^b$, see Eq. 6) as a function of x in the same two phases; curve (c) is the total hydrogen concentration. **c.** Phase-normalized hydrogen concentrations ($x_i = n_i^b / N_i^b$, see Eq. 9) as a function of x.

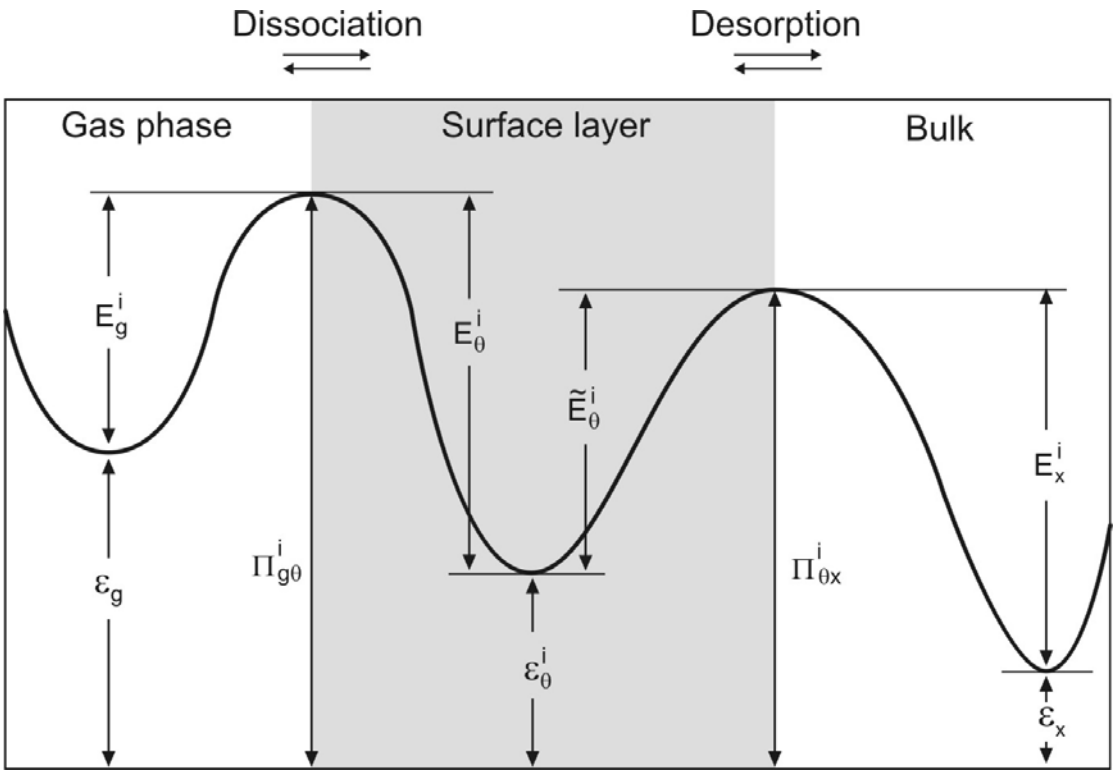

FIG. 4. Energy diagram of the various hydrogen species involved in the (de)hydrogenation system defined in Fig. 2, including the energies of atomic hydrogen in the gas phase (ε_g), at the surface (ε_θ) and in the bulk (ε_x), the various activation energies (E_m^i) and energy barriers (Π_m^i). All energies are given with respect to an arbitrary chosen reference state.

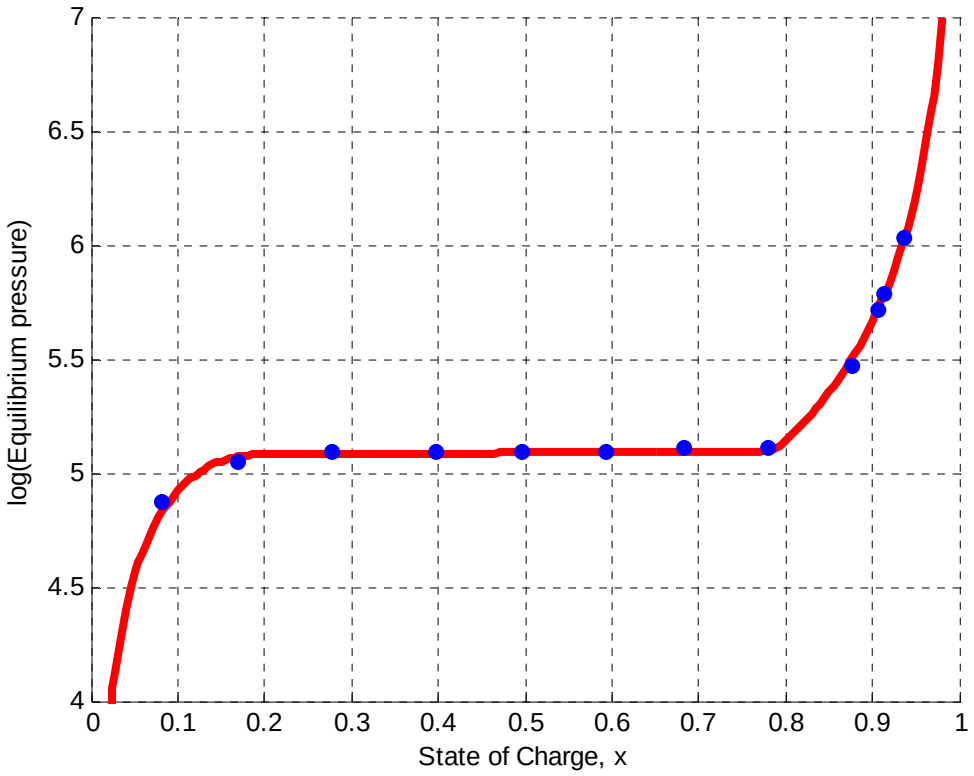

FIG.8. Measured (symbols) and calculated (line) pressure-composition isotherm for the stoicheometric alloy $LaNi_{4.0}Cu_{1.0}$. The measurements have been performed via the gas phase 20 ºC[4,19].

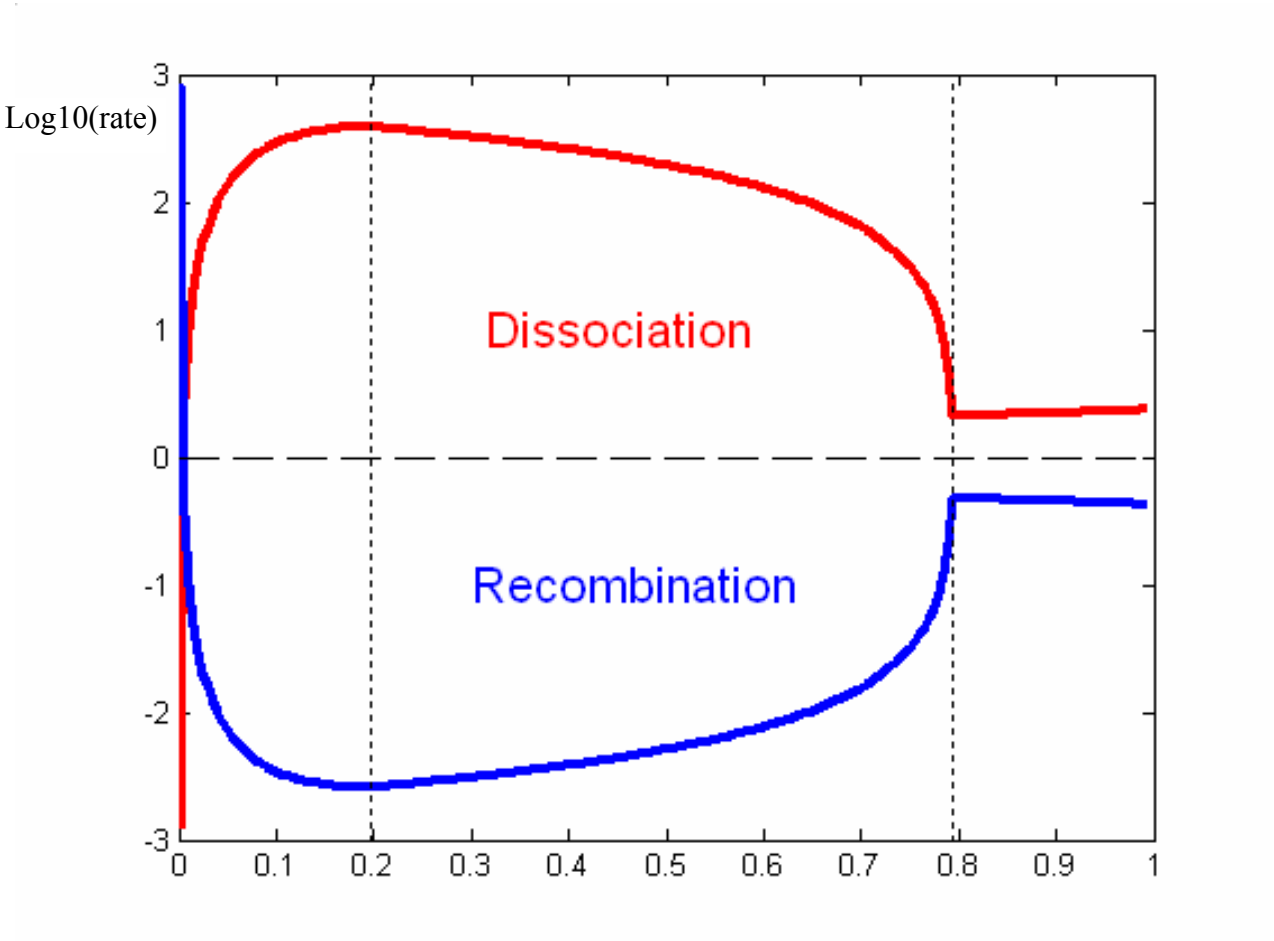

FIG.9. Dissociation and recombination rates in equilibrium conditions for stoichiometric alloy $LaNi_{4.0}Cu_{1.0}$.

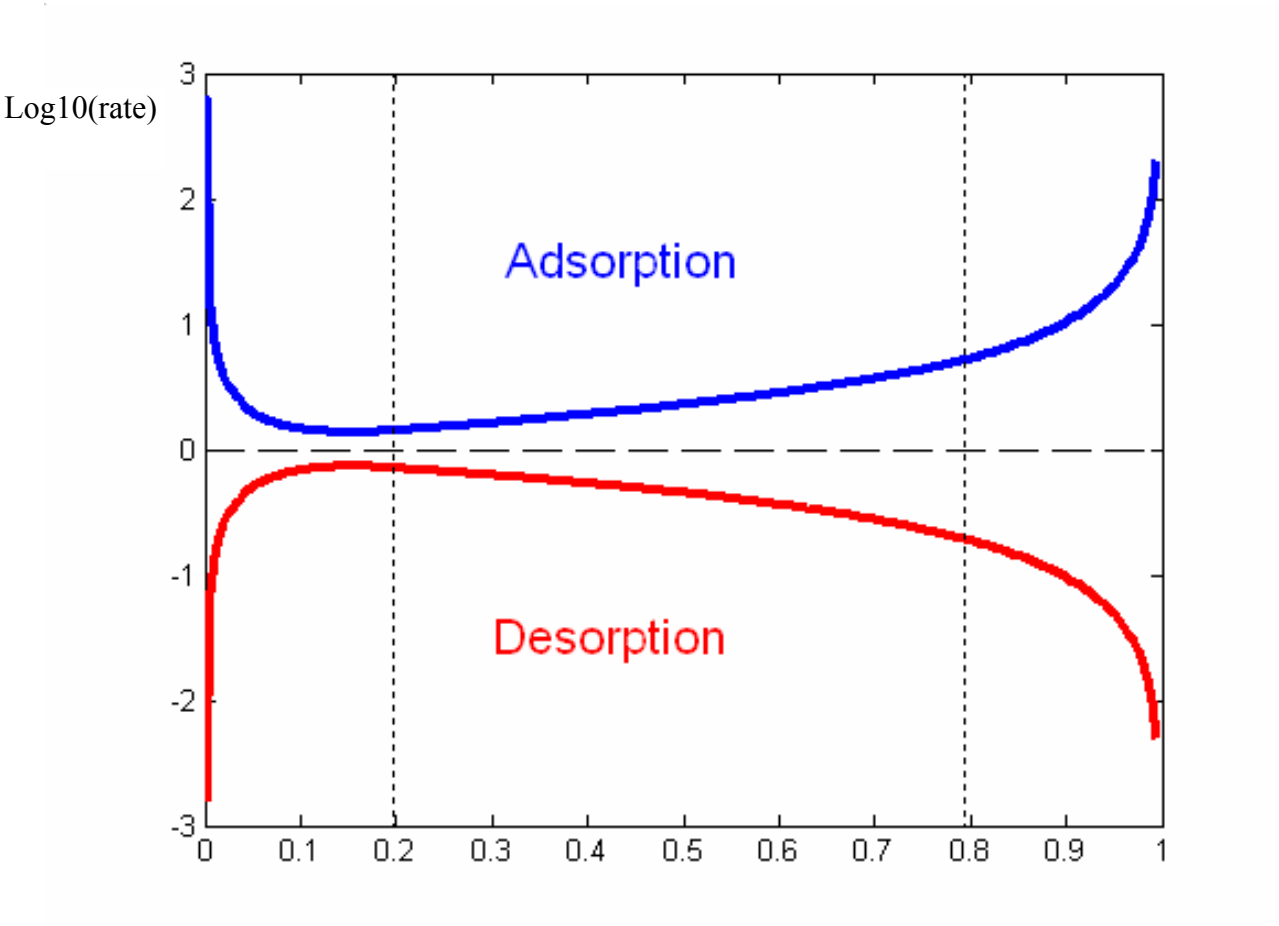

FIG.10. Absorption and desorption rates in equilibrium conditions for stoichiometric alloy $LaNi_{4.0}Cu_{1.0}$.

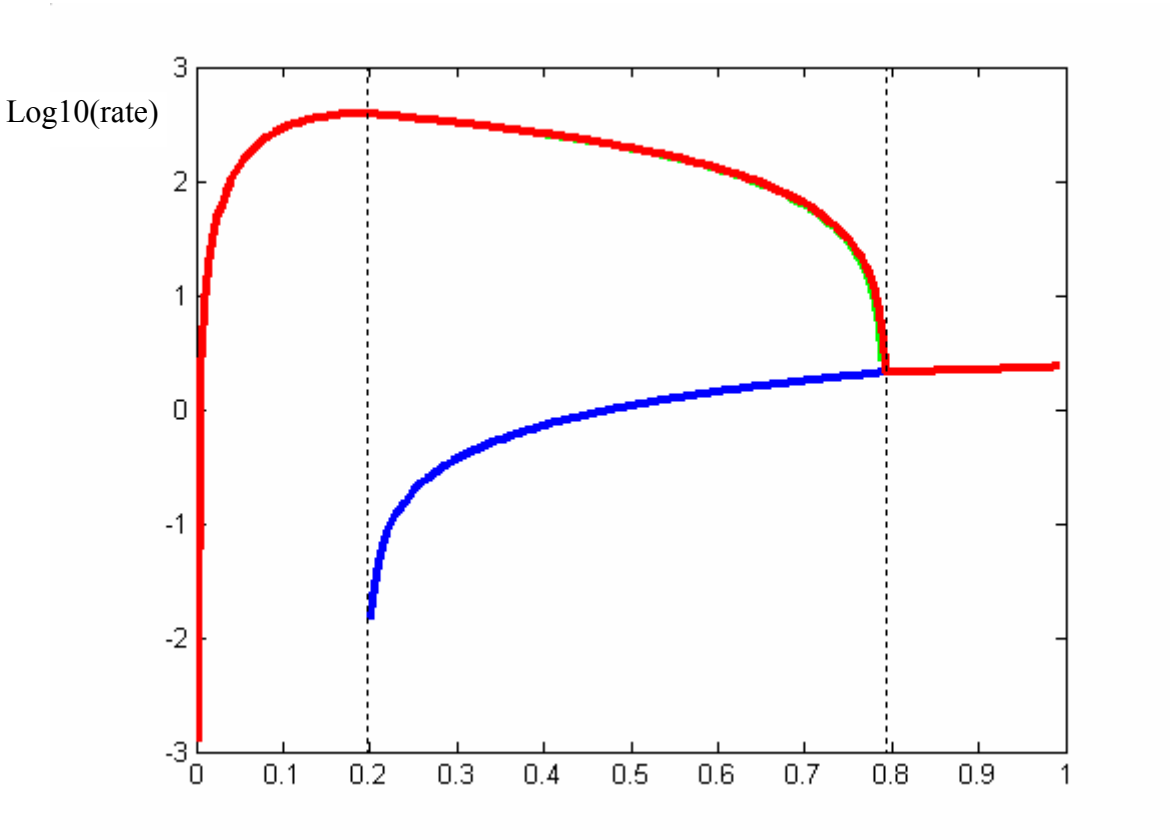

FIG.11. Composition of the dissociation rate in equilibrium conditions for stoichiometric alloy $LaNi_{4.0}Cu_{1.0}$.

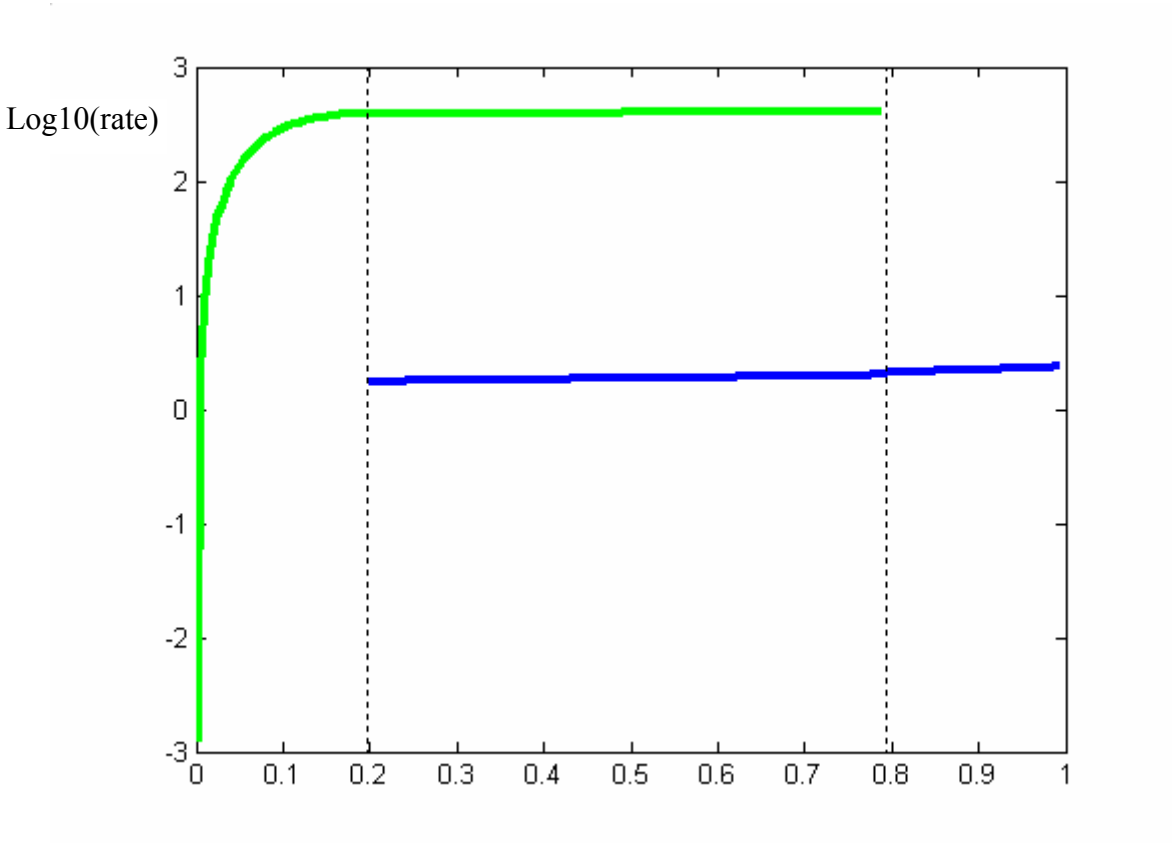

FIG.12. Normalized dissociation rates in equilibrium conditions for stoichiometric alloy $LaNi_{4.0}Cu_{1.0}$.

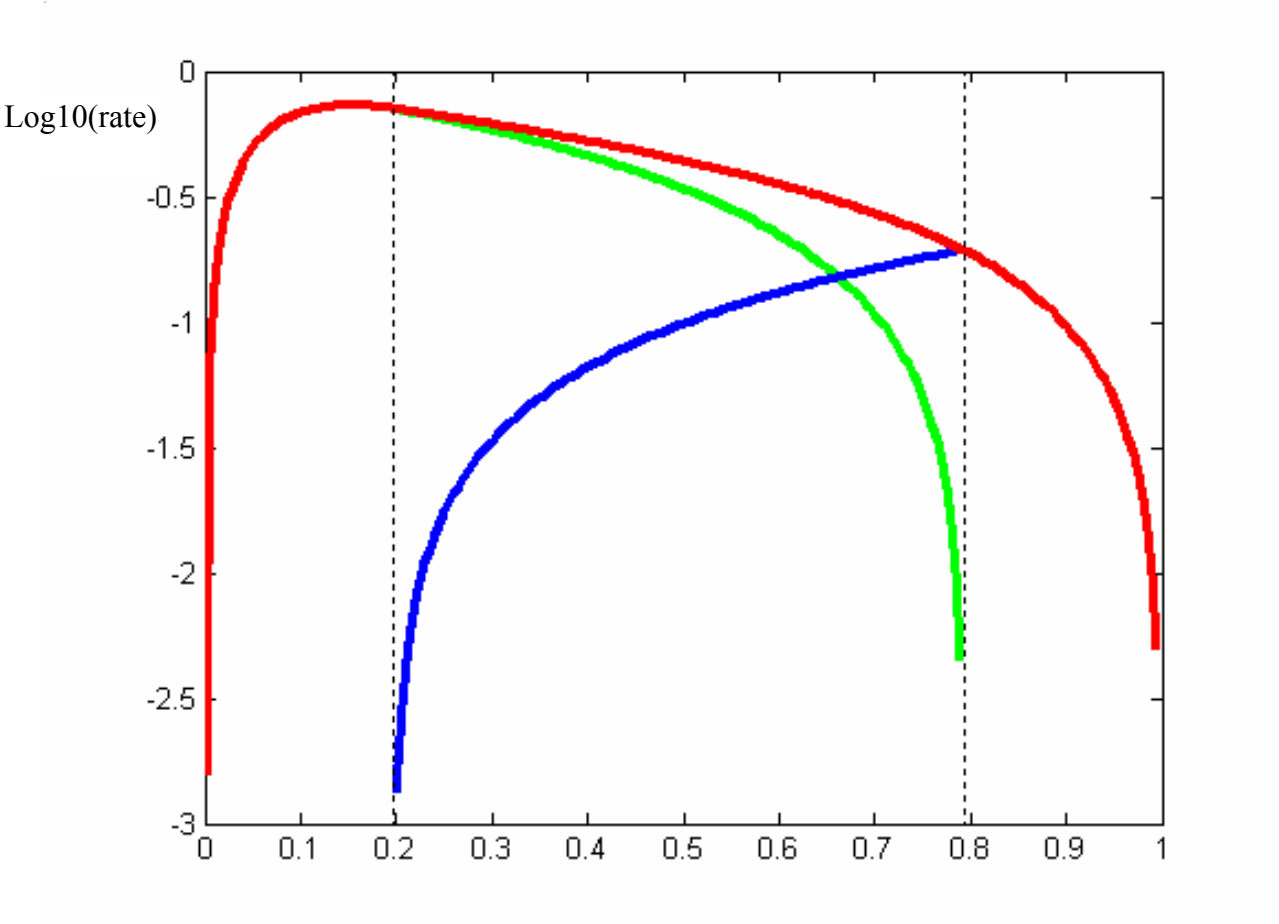

FIG.13. Composition of the absorption rate in equilibrium conditions for stoichiometric alloy $LaNi_{4.0}Cu_{1.0}$.

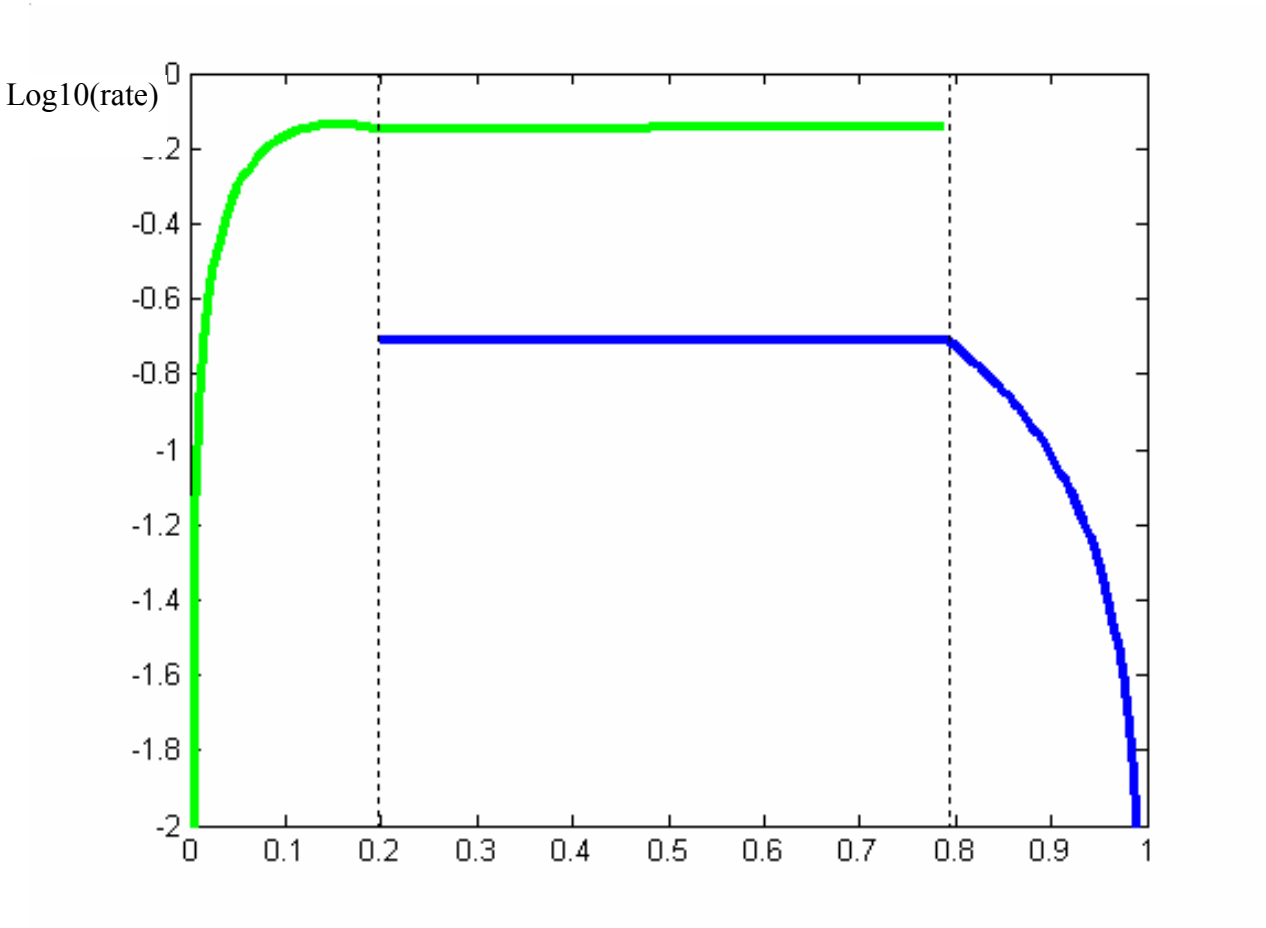

FIG.14. Normalized absorption rates in equilibrium conditions for stoichiometric alloy $LaNi_{4.0}Cu_{1.0}$.

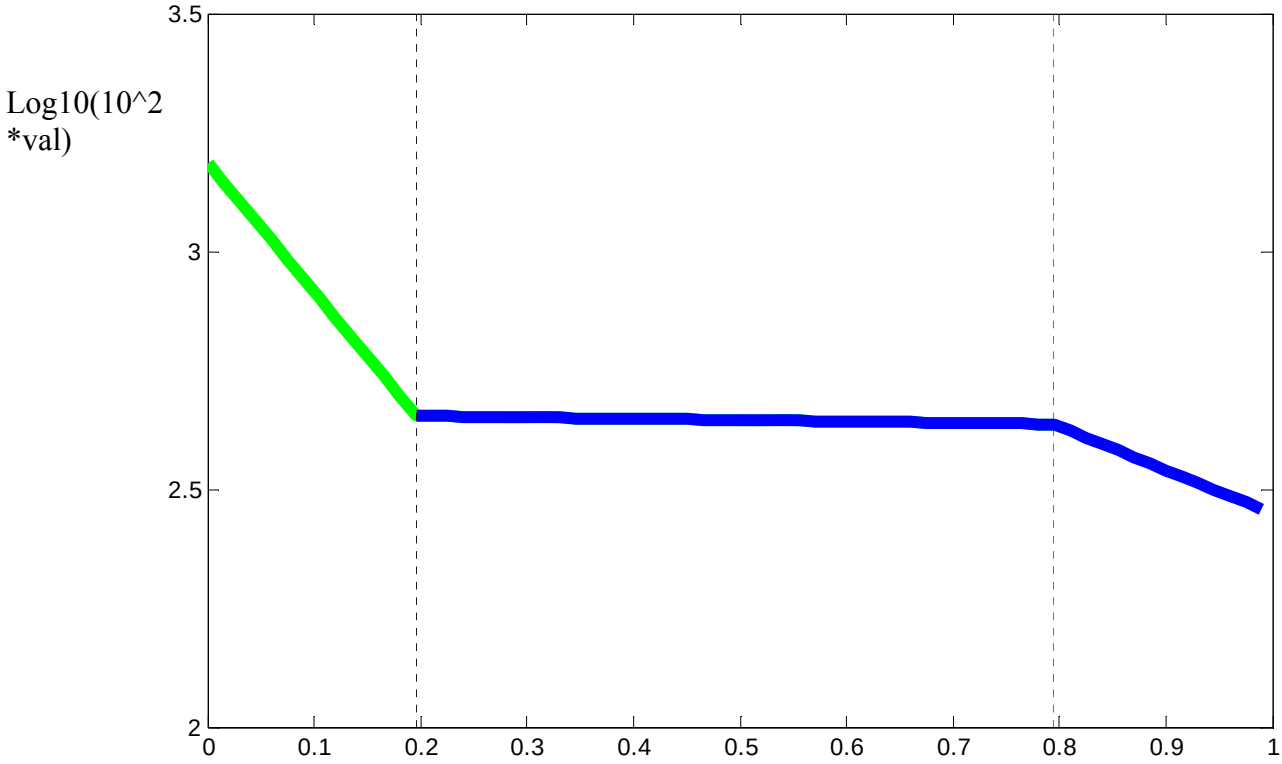

FIG.15. Desorption rate constant in equilibrium conditions for stoichiometric alloy $LaNi_{4.0}Cu_{1.0}$.

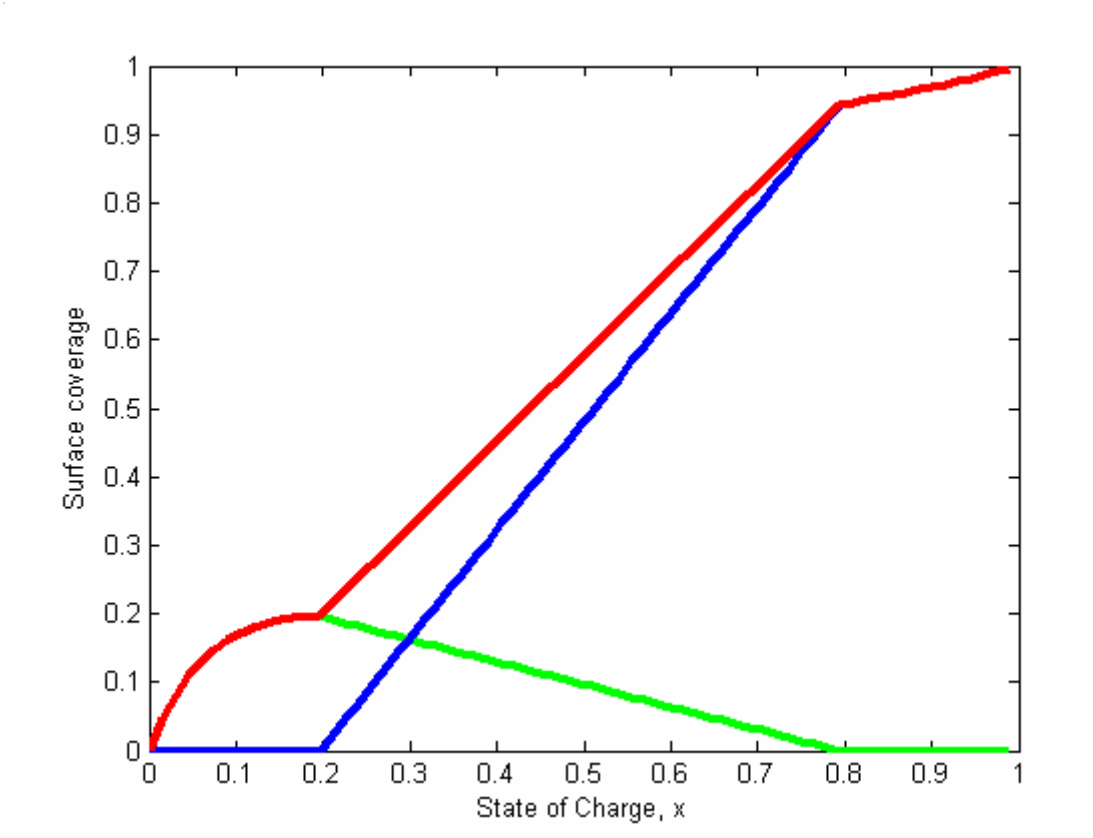

FIG.16. Surface coverages for stochiometric alloy $LaNi_{4.0}Cu_{1.0}$. Blue line is the surface coverage of the α phase ($\theta^{\alpha}(x)$), green line is the surface coverage of the β phase ($\theta^{\beta}(x)$), red line is the total surface coverage ($\theta(x)=\theta^{\alpha}(x)+\theta^{\beta}(x)$).

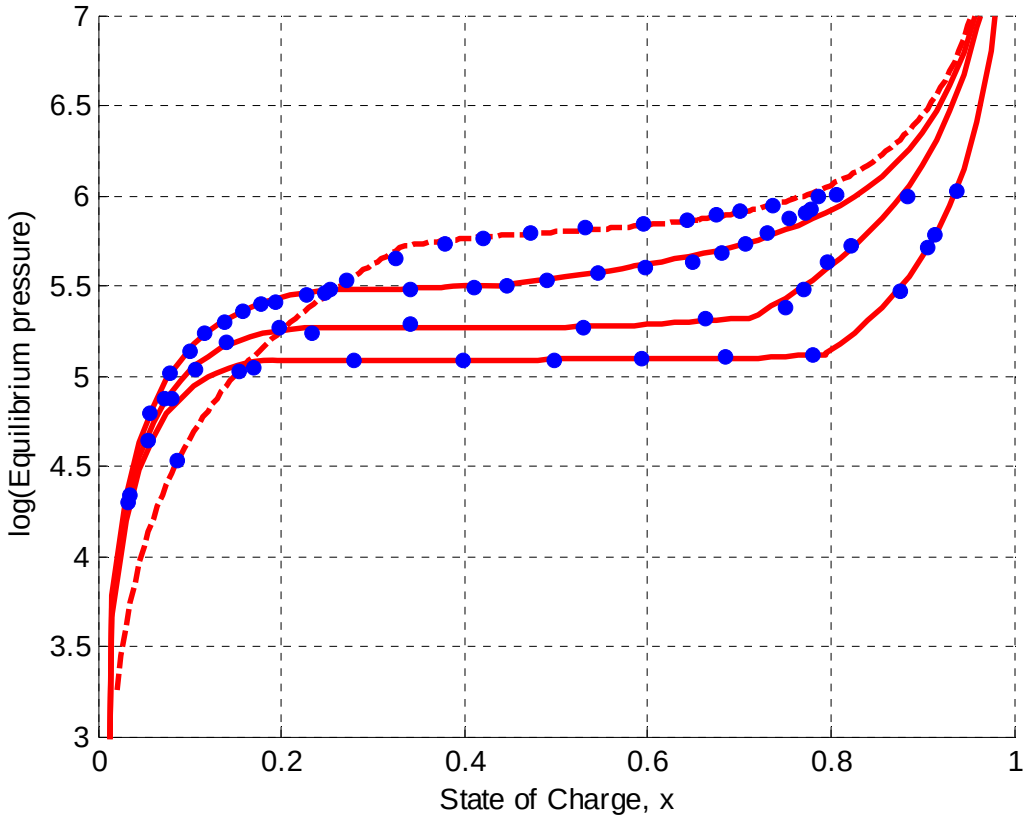

FIG.17. Measured (symbols) and calculated (lines) pressure-composition isotherms for various (non)stoichiometric compounds as a function of composition: $LaNi_{4.0}Cu_{1.0}$ (a), $LaNi_{4.2}Cu_{1.0}$ (b), $LaNi_{4.4}Cu_{1.0}$ (c), $LaNi_{5.0}Cu_{1.0}$ (d). All measurements have been performed via the gas phase 20 ºC[19].

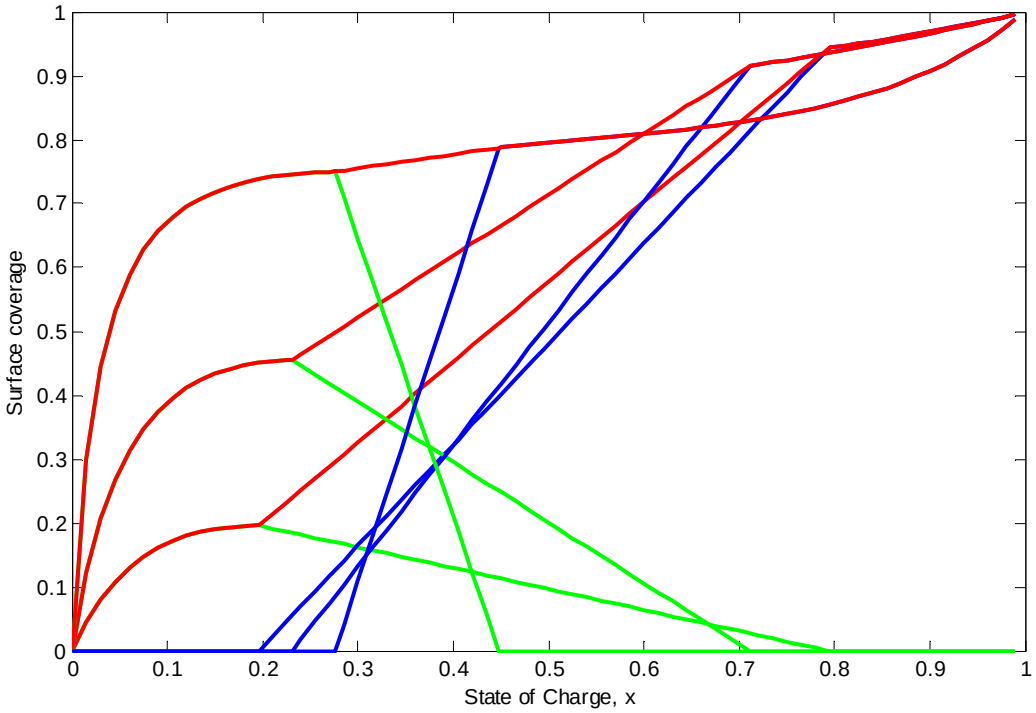

FIG.18. Surface coverages for all (non)stochiometric alloys $LaNi_xCu_{1.0}$.

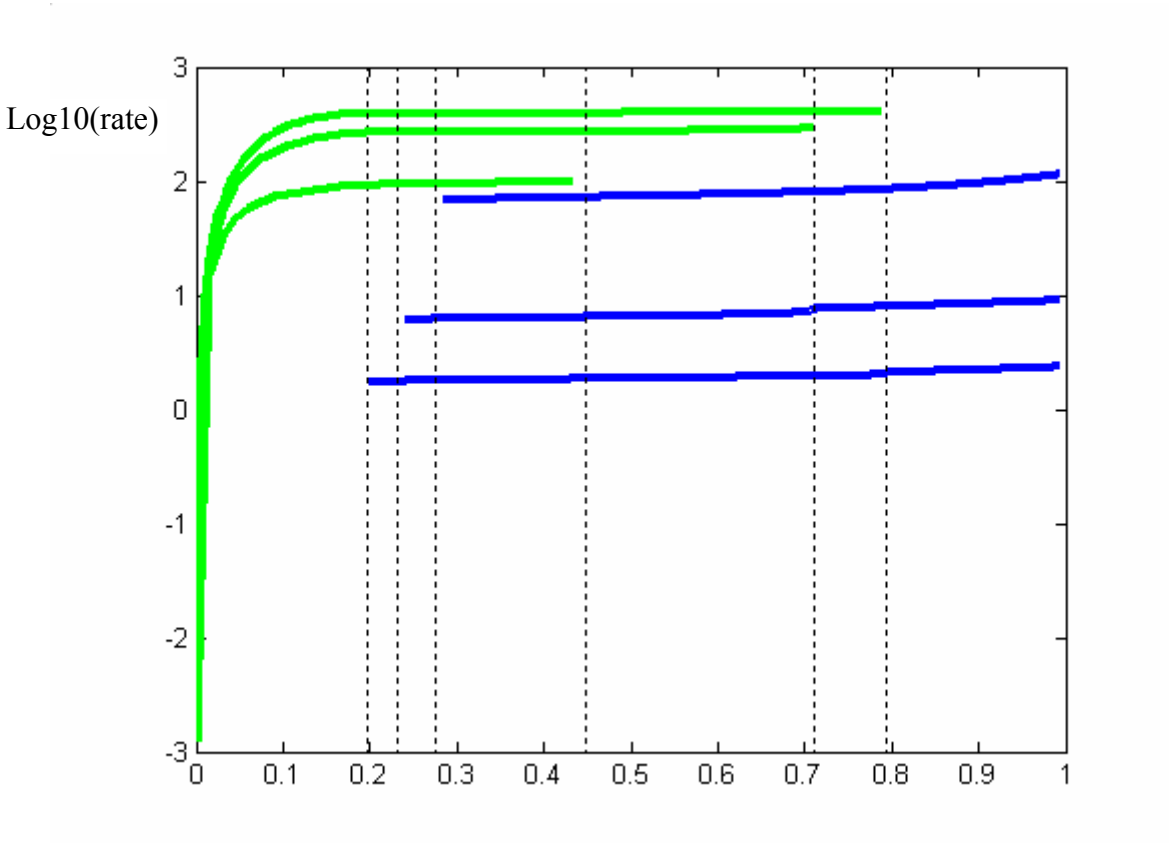

Fig.19. Normalized recombination rates for stochiometric alloys $LaNi_xCu_{1.0}$.

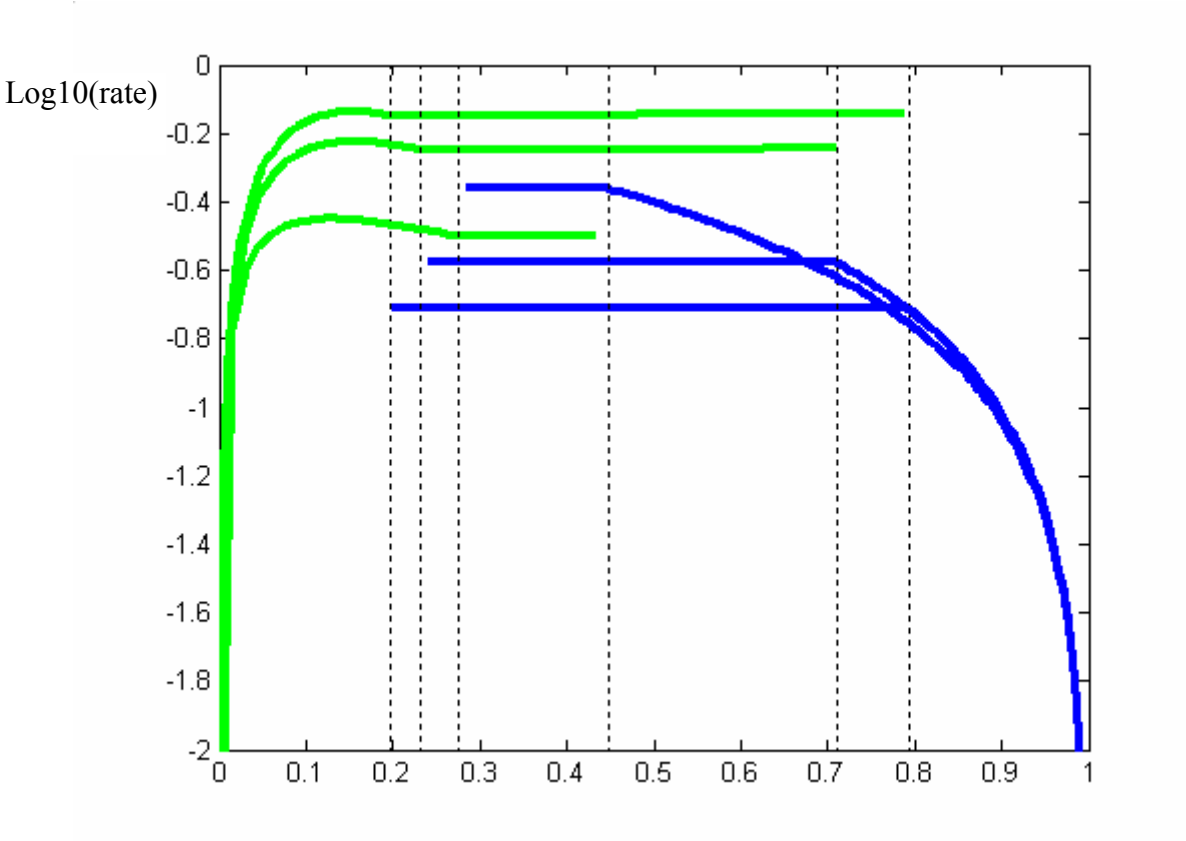

Fig.20. Normalized absorption rates for stochiometric alloys $LaNi_xCu_{1.0}$.

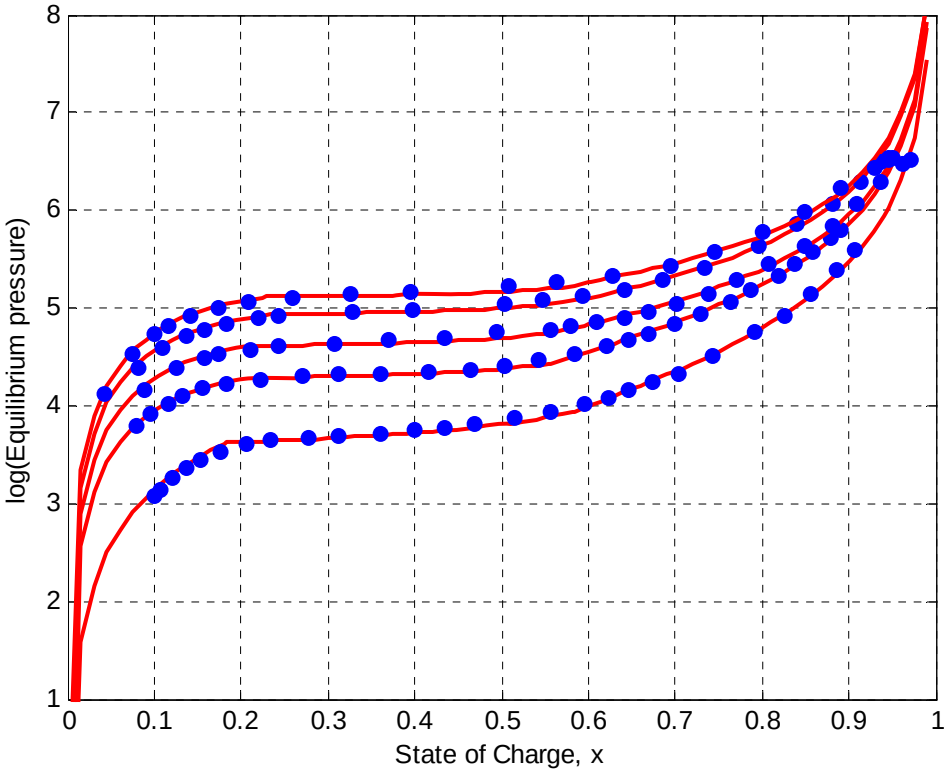

FIG.21. Pressure-composition isotherms for a commercial, MischMetal-based, hydride-forming electrode material at 0 (a), 24 (b), 45 (c) 60 (d) and 70 ºC (e)[30,31].

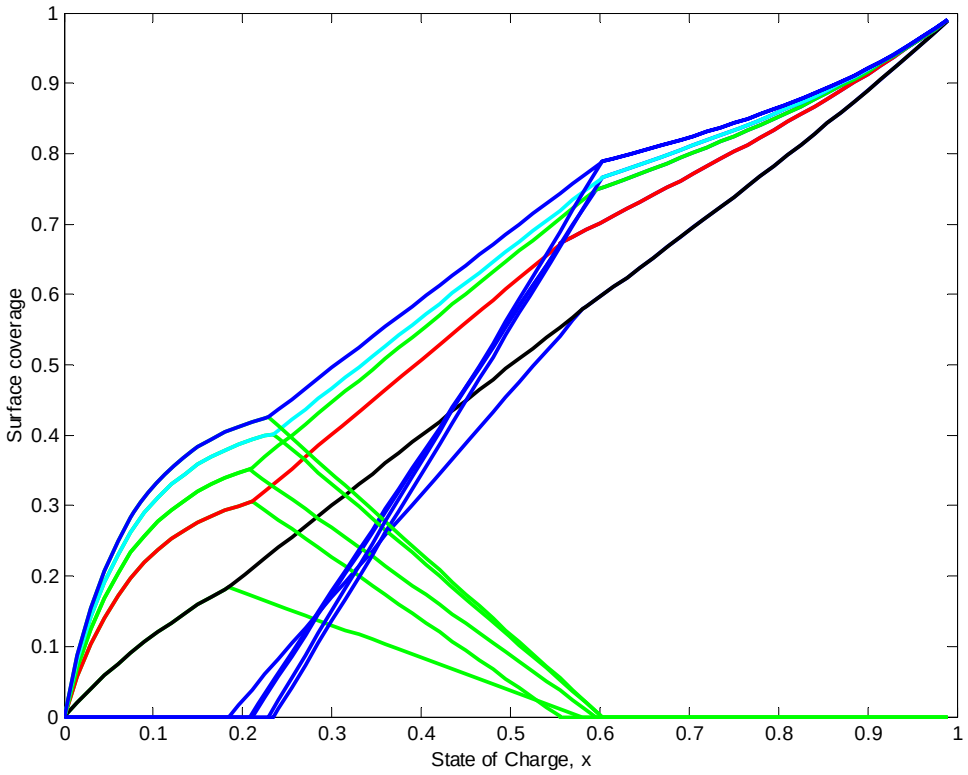

FIG.22. Surface coverages for a commercial, MischMetal-based, hydride-forming electrode material: 0C is black line; 24C is red line; 45C is green line; 60C is cyan line; 70C is blue line.

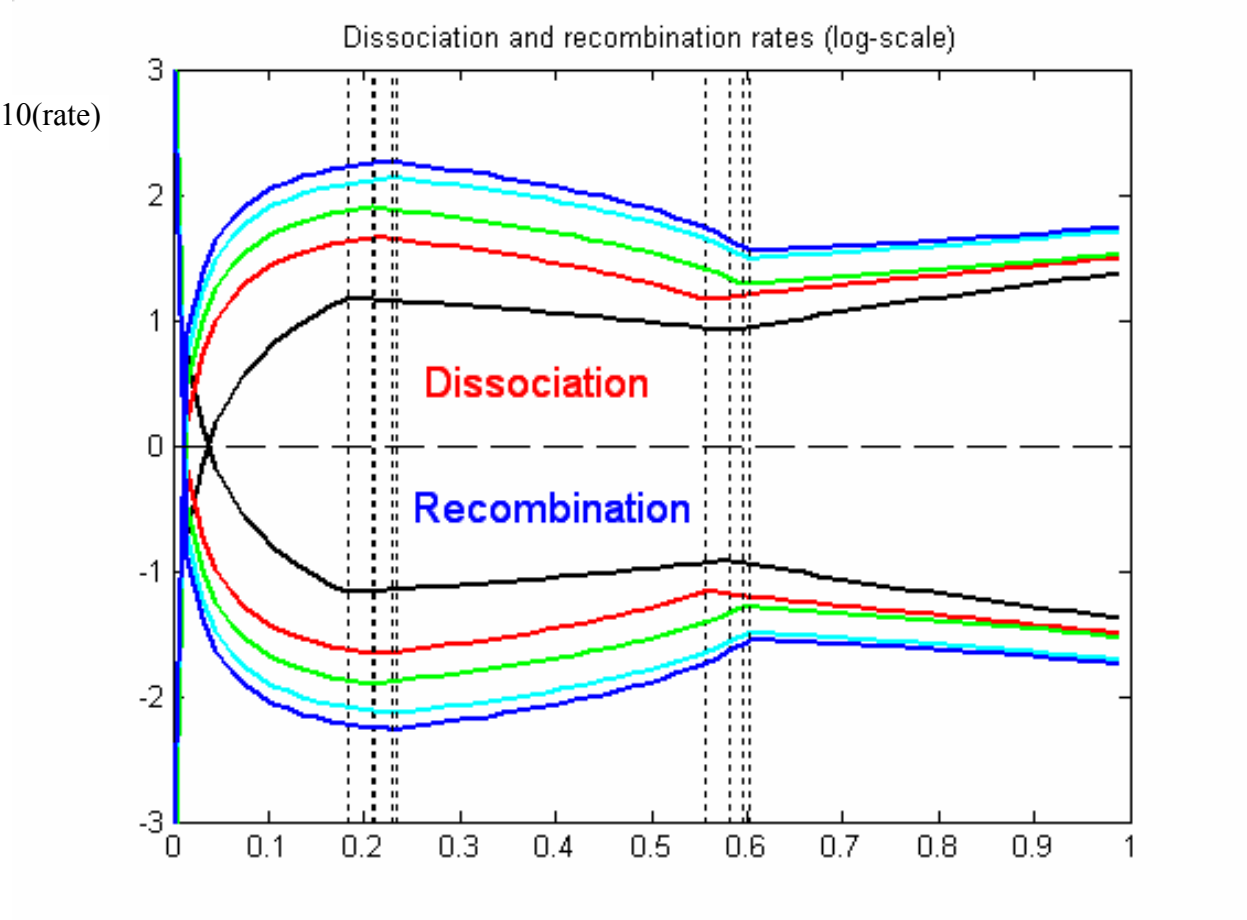

FIG.23. Dissociation and recombination rates for a commercial, MischMetal-based, hydride-forming electrode material in equilibrium conditions as function of temperature: 0C is black line; 24C is red line; 45C is green line; 60C is cyan line; 70C is blue line.

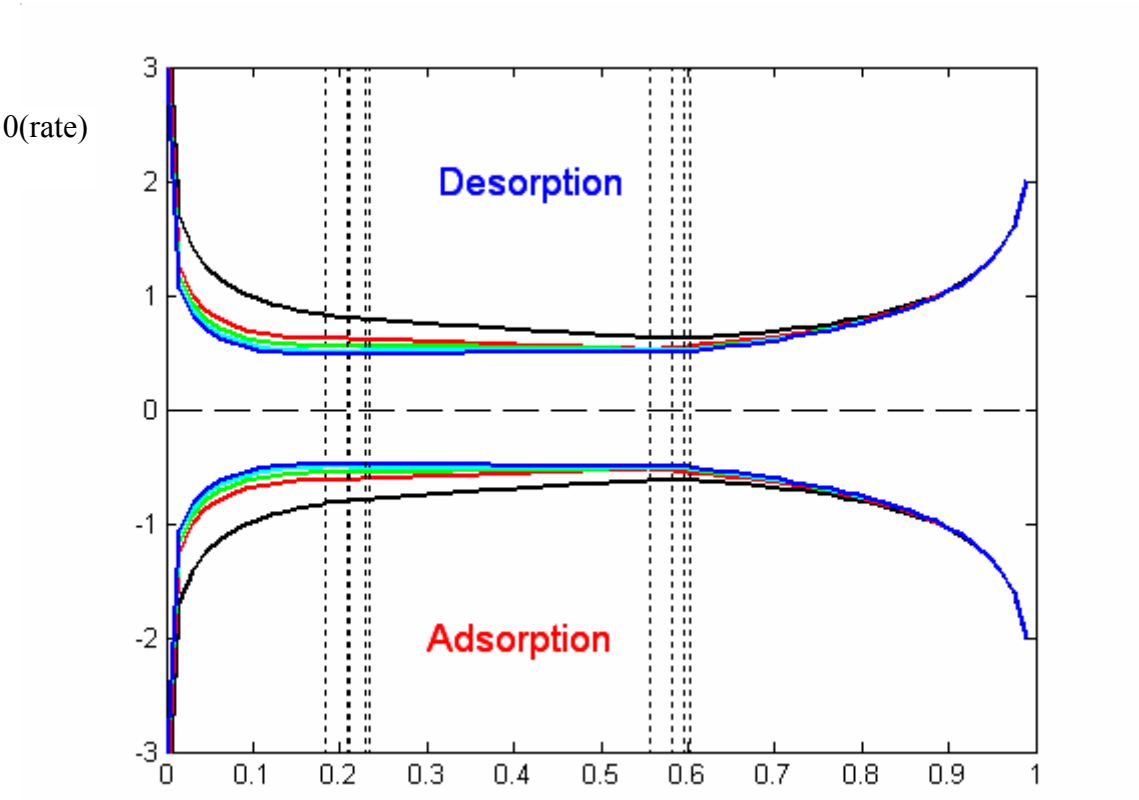

FIG.24. Absorption and desorption rates for a commercial, MischMetal-based, hydride-forming electrode material in equilibrium conditions as function of temperature: 0C is black line; 24C is red line; 45C is green line; 60C is cyan line; 70C is blue line.

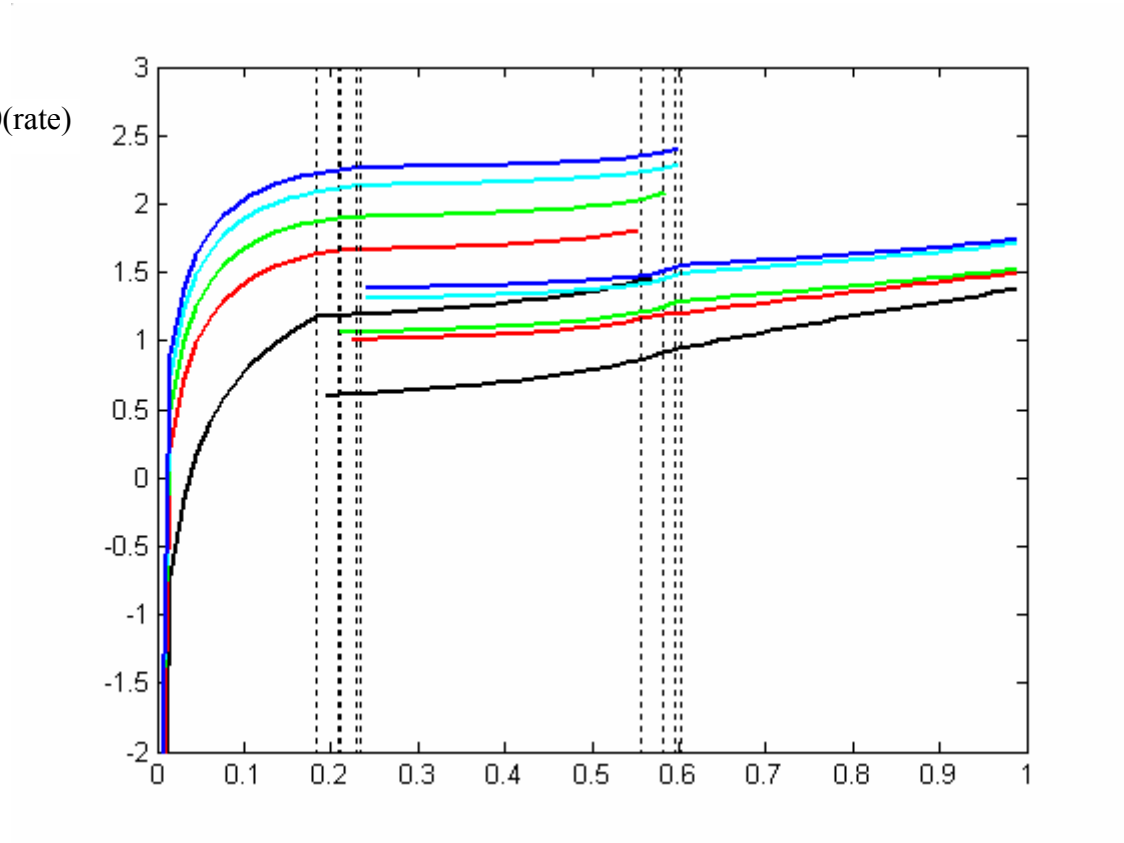

FIG.25. Normalized recombination rates for a commercial, MischMetal-based, hydride-forming electrode material in equilibrium conditions as function of temperature: 0C is black line; 24C is red line; 45C is green line; 60C is cyan line; 70C is blue line.

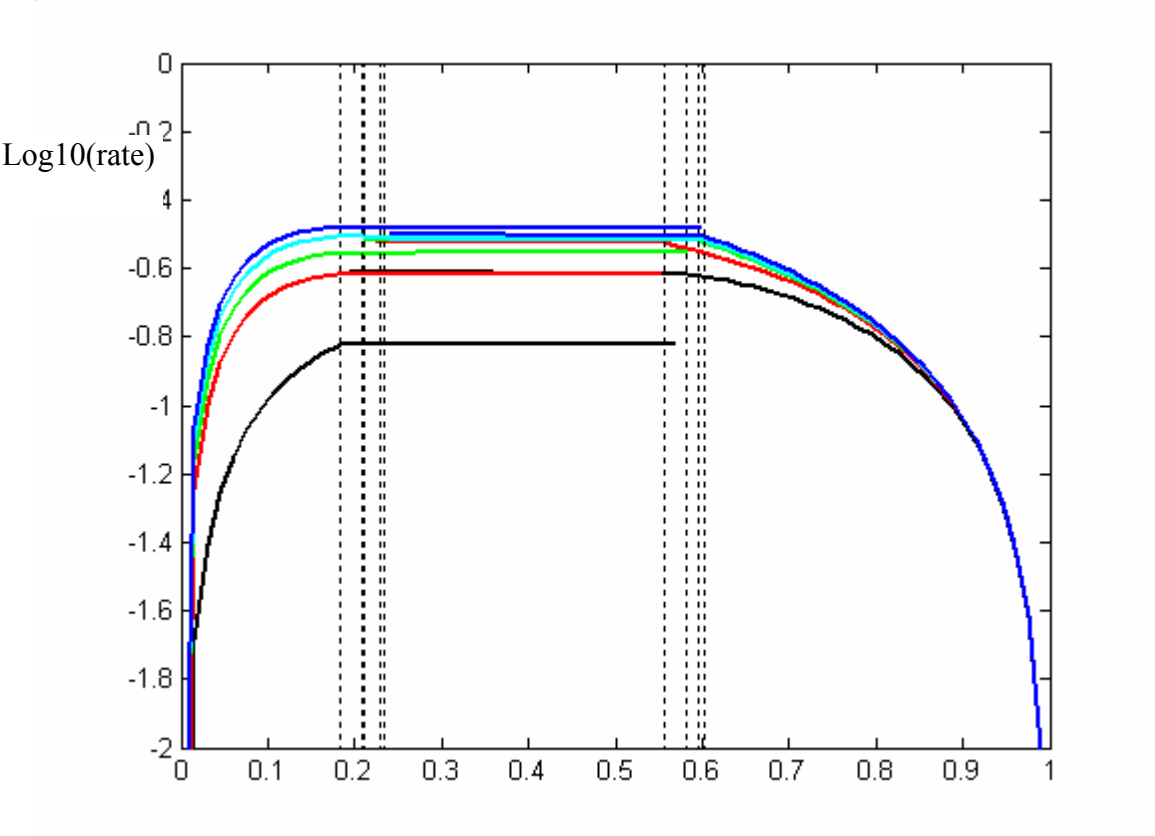

FIG.26. Normalized absorption rates for a commercial, MischMetal-based, hydride-forming electrode material in equilibrium conditions as function of temperature: 0C is black line; 24C is red line; 45C is green line; 60C is cyan line; 70C is blue line.

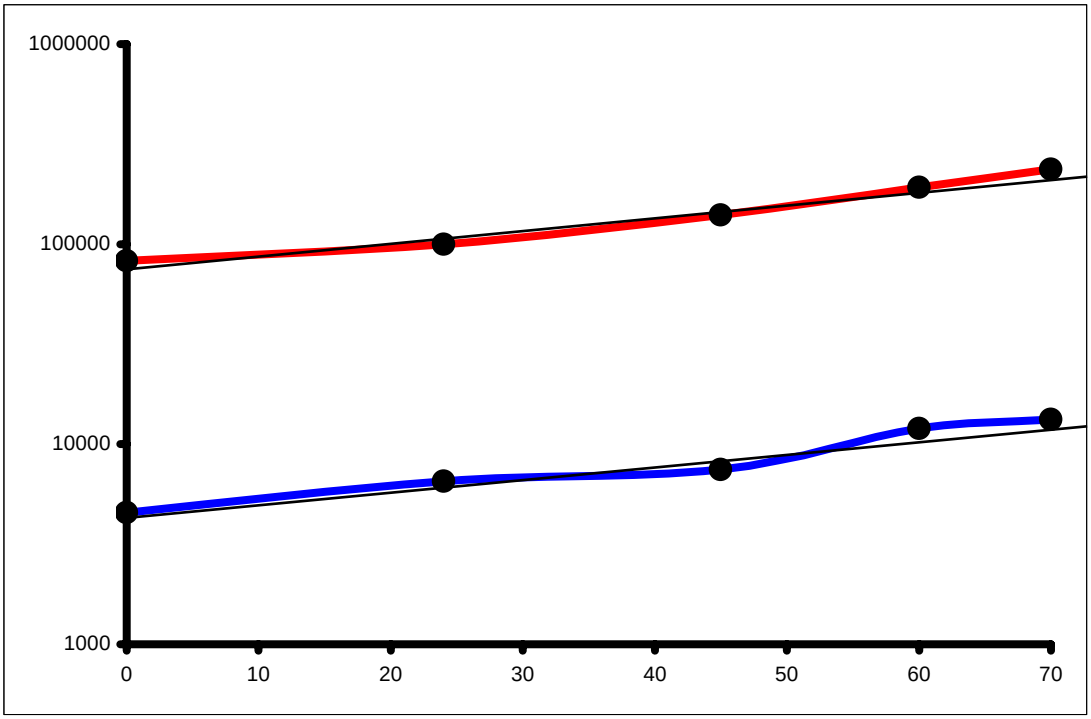

FIG.27. Behavior of parameters $P^{(\alpha)}$ and $P^{(\beta)}$ as functions of temperature for MischMetal-based, hydride-forming electrode material.